

# Characterization of the Copper–Sulfur Chromophores in Nitrous Oxide Reductase by Resonance Raman Spectroscopy: Evidence for Sulfur Coordination in the Catalytic Cluster

Marcela L. Alvarez,<sup>†</sup> Jingyuan Ai,<sup>‡</sup> Walter Zumft,<sup>§</sup> Joann Sanders-Loehr,<sup>\*,‡</sup> and David M. Dooley<sup>\*,†</sup>

Contribution from the Department of Chemistry and Biochemistry, Montana State University, Bozeman, Montana 59717, Lehrstuhl für Mikrobiologie, Universität Fridericiana, D-76228 Karlsruhe, Germany, and Department of Biochemistry and Molecular Biology, Oregon Graduate Institute of Science and Technology, Beaverton, Oregon 97006-8921

Received December 9, 1999. Revised Manuscript Received September 19, 2000

**Abstract:** Nitrous oxide reductase (N<sub>2</sub>OR) from *Pseudomonas stutzeri*, a dimeric enzyme with a canonical metal ion content of at least six Cu ions per subunit, contains two types of multinuclear copper sites: Cu<sub>A</sub> and Cu<sub>Z</sub>. An electron-transfer role for the dinuclear Cu<sub>A</sub> site is indicated based on its similarity to the Cu<sub>A</sub> site in cytochrome *c* oxidase (CcO), a dicysteinate-bridged, mixed-valence cluster. The Cu<sub>Z</sub> site is the catalytic site, which had long been thought to have novel spectroscopic properties. However, the low-energy electronic transitions and resonance Raman features attributable to Cu<sub>Z</sub> have been difficult to reconcile with a lack of conserved cysteine residues in standard alignments of N<sub>2</sub>OR sequences, other than those associated with the Cu<sub>A</sub> site. Recent evidence indicates that nitrous oxide reductase contains acid-labile sulfide and that this sulfide is a constituent of the Cu<sub>Z</sub> site (Rasmussen, T.; Berks, B. C.; Sanders-Loehr, J.; Dooley, D. M.; Zumft, W. G.; Thomson, A. J. *Biochemistry* 2000, 39, 12753–12756). We have used resonance Raman (RR) spectroscopy to selectively probe the Cu<sub>A</sub> and Cu<sub>Z</sub> sites of N<sub>2</sub>OR in three oxidation states (oxidized, semireduced, and reduced) as well as Cu<sub>A</sub>-only and Cu<sub>Z</sub>-only variants. The Cu<sub>A</sub> (mixed-valence, also designated as A<sub>mv</sub>) RR spectrum exhibits 10 vibrational modes between 220 and 410 cm<sup>-1</sup>, with >1-cm<sup>-1</sup> <sup>34</sup>S isotope shifts that sum to -16.6 cm<sup>-1</sup>. Many of these modes are also sensitive to <sup>65</sup>Cu and <sup>15</sup>N(His) and, thus, can be assigned to coupling of the Cu–S stretch, ν(Cu–S), with cysteine and histidine vibrations of the Cu<sub>2</sub>Cys<sub>2</sub>His<sub>2</sub> core. The RR spectrum of the Cu<sub>Z</sub> site (Z<sub>ox</sub>) reveals a novel Cu–sulfur chromophore with four S isotope-sensitive modes at 293, 347, 352, and 408 cm<sup>-1</sup>, with a total <sup>34</sup>S shift of -19.9 cm<sup>-1</sup>. The magnitude of the S isotope shifts and wide spread of perturbed frequencies are similar to those observed in Cu<sub>A</sub> and therefore suggest a sulfur-bridged cluster in Z<sub>ox</sub>. The Z<sub>ox</sub> site has its ν(Cu–S)-containing modes at higher energy and exhibits less mixing with ligand deformations, compared to Cu<sub>A</sub>. Reduction by dithionite produces a mixed-valence Cu<sub>Z</sub> site (Z<sub>mv</sub>) with six S isotope-sensitive RR modes between 282 and 382 cm<sup>-1</sup> and a total <sup>34</sup>S-shift of -16.9 cm<sup>-1</sup>. The observation of a nearly identical RR spectrum in the C622D variant of N<sub>2</sub>OR, which lacks one of the conserved Cu<sub>A</sub> Cys residues, establishes that Cu–S vibrations observed in this variant arise from the Z<sub>mv</sub> site. Furthermore, none of the features assigned to Cu<sub>Z</sub> are detected in a second variant that contains only Cu<sub>A</sub>. Therefore the resonance Raman spectra reported here provide compelling evidence for a unique Cu–S cluster in the catalytic site of nitrous oxide reductase.

## Introduction

Denitrification, the process by which nitrate is converted to dinitrogen by many soil and marine bacteria, is a key component of the global nitrogen cycle.<sup>1–3</sup> All four steps in this pathway (eq 1) are catalyzed by metalloproteins. In addition, the



enzymatic reduction of nitrate, nitrite, and nitrous oxide is coupled to ATP synthesis via proton translocation and the formation of a membrane potential, thereby constituting anaerobic respiration in these microorganisms. Nitrous oxide reductase (N<sub>2</sub>OR) catalyzes the terminal step of denitrification, which is the two-electron reduction of nitrous oxide to water and dinitrogen (eq 2).

The recent X-ray crystal structure of *Pseudomonas nautica* nitrous oxide reductase<sup>4</sup> revealed the presence of two distinct multinuclear copper sites: a dinuclear, dithiolate-bridged cluster, essentially identical to the structurally characterized Cu<sub>A</sub> site in cytochrome oxidase; and a novel tetranuclear copper cluster,

\* To whom correspondence should be addressed: (phone) (406) 994-4801; (fax) (406) 994-5407; (e-mail) dmdooley@montana.edu.

<sup>†</sup> Montana State University.

<sup>‡</sup> Oregon Graduate Institute of Science and Technology.

<sup>§</sup> Universität Fridericiana.

(1) Zumft, W. G.; Viebrock, A.; Körner, H. In *The Nitrogen and Sulfur Cycles*; Cole, J. A., Ferguson, S. J., Eds.; Cambridge University Press: Cambridge, U.K., 1988; p 245.

(2) Berks, B. C.; Ferguson, S. J.; Moir, J. W. B.; Richardson, D. J. *Biochim. Biophys. Acta* 1995, 1232, 97–173.

(3) Zumft, W. G. *Microbiol. Mol. Biol. Rev.* 1997, 61, 533–616.

(4) Brown, K.; Tegoni, M.; Prudêncio, M.; Pereira, A. S.; Besson, S.; Moura, J. J.; Moura, I.; Cambillau, C. *Nat. Struct. Biol.* 2000, 7, 191–195.

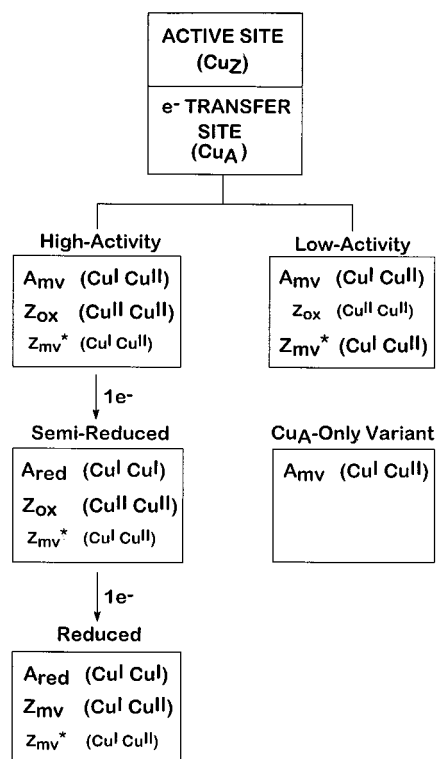


**Figure 1.** Oxidation states of Cu<sub>A</sub> and Cu<sub>Z</sub> sites in different forms of N<sub>2</sub>OR. Only two of the four copper ions in the tetranuclear Cu<sub>Z</sub> cluster are indicated. The dinuclear A species appear to have bridging cysteine thiolate ligands and are located at the electron-transfer site, whereas all of the multinuclear Z species are bridged by sulfide<sup>22</sup> and are located at the active site.

which is the first example of such a catalytic copper cluster in biology. The crystal structure is that of the reduced state, characterized by an absorption band at ~640–650 nm at 100 K. Notably, the current crystallographic model for the catalytic cluster features seven histidine imidazole ligands and three ligands modeled as water or hydroxide distributed over the four copper ions.

Spectroscopic data, including multifrequency EPR,<sup>5–9</sup> ENDOR,<sup>10</sup> EXAFS,<sup>11,12</sup> magnetic circular dichroism (MCD),<sup>7,11–13</sup> and resonance Raman (RR) data<sup>14,15</sup> on the native, high-activity enzyme, had been interpreted in terms of two multinuclear copper sites: Cu<sub>Z</sub> and Cu<sub>A</sub> (Figure 1). The dinuclear Cu<sub>A</sub> sites

in nitrous oxide reductase and cytochrome *c* oxidase (CcO) are mixed-valence [Cu(1.5)•Cu(1.5)] units with two bridging cysteine thiolates, two terminal histidines, and a Cu–Cu distance of 2.5 Å.<sup>16,17</sup> In analogy to the established electron-transfer function of Cu<sub>A</sub> in CcO, Cu<sub>A</sub> in N<sub>2</sub>OR is presumed to transfer electrons from the physiological donor to substrate bound in the catalytic site. The spectral features of the mixed-valence Cu<sub>A</sub> in N<sub>2</sub>OR have been documented and analyzed in considerable detail. In addition, an oxidized copper cluster has been detected in N<sub>2</sub>OR that exhibits diamagnetic behavior, absorption bands at 570 and 650 nm, a copper–sulfur RR spectrum, and low-energy, intense circular dichroism (CD) and MCD transitions.<sup>7,12,14,18,19</sup> These spectral features were consistent with the presence of strongly antiferromagnetically coupled [Cu(II)•Cu(II)] centers with at least one coordinated sulfur anion (originally presumed to be cysteine) and were initially correlated to an oxidized form of the catalytic site, Cu<sub>Z</sub>. Reduced N<sub>2</sub>OR displays an absorption band at ~650 nm and a broad *S* = 1/2 EPR signal previously attributed to a mixed-valence state of Cu<sub>Z</sub>. Cu<sub>Z</sub> was formulated as an independent, multinuclear site responsible for the reduction of N<sub>2</sub>O. However, standard alignments of N<sub>2</sub>OR sequences from six sources reveal no fully conserved cysteines other than the two known Cu<sub>A</sub> ligands.<sup>20,21</sup> A major step toward the resolution of the nature of Cu<sub>Z</sub> is the very recent finding that N<sub>2</sub>OR contains inorganic sulfide, at an apparent stoichiometry of 1S<sup>2-</sup>/subunit.<sup>22</sup> This finding led to the proposal that Cu<sub>Z</sub> is the first example of a biological copper–sulfide cluster. Here we report detailed resonance Raman spectra that fully support this proposal and establish that Cu<sub>Z</sub> is a copper–sulfur chromophore.

Elucidation of the copper centers in N<sub>2</sub>OR has been facilitated by examining three oxidation states of the enzyme, i.e., native, semireduced, and reduced, as well as an enzymatically inactive Cu<sub>A</sub>-only variant (previously designated N<sub>2</sub>OR V), and a Cu<sub>Z</sub>-only variant (produced by the C622D mutation). (Different forms of N<sub>2</sub>OR from *P. stutzeri* have previously been abbreviated, in ref 4, as follows: N<sub>2</sub>OR I, high-activity native enzyme obtained from anaerobic purification; N<sub>2</sub>OR II, low-activity native enzyme obtained from aerobic purification; N<sub>2</sub>OR III, dithionite-reduced enzyme; N<sub>2</sub>OR V, Cu<sub>A</sub>-only mutant obtained from a strain defective in the biosynthesis of the catalytic site.) Native N<sub>2</sub>OR can be isolated anaerobically in a high-activity “purple” form (previously designated N<sub>2</sub>OR I) or aerobically in a low-activity “pink” form (previously designated N<sub>2</sub>OR II).<sup>5</sup> Both forms display a distinctive seven-line EPR signal that has been attributed to a delocalized unpaired electron in the Cu<sub>A</sub> site (A<sub>mv</sub>, Figure 1).<sup>9</sup> This mixed-valence site also dominates the absorption spectrum, with a prominent band at 540 nm, a shoulder at 480 nm, and a weaker transition at 780 nm (Figure 2). The Cu<sub>Z</sub> site in the native enzyme appears to be present in two states, designated Z<sub>ox</sub> and Z<sub>mv</sub>\* (Figure 1). While high-activity enzyme contains mainly diamagnetic Z<sub>ox</sub>, evidence for the mixed-valence form (Z<sub>mv</sub>\*) is manifested as a weak, broad

(5) Riester, J.; Zumft, W. G.; Kroneck, P. M. H. *Eur. J. Biochem.* **1989**, *178*, 751–762.

(6) Neese, F.; Zumft, W. G.; Antholine, W. E.; Kroneck, P. M. H. *J. Am. Chem. Soc.* **1996**, *118*, 8692–8699.

(7) Farrar, J. A.; Thomson, A. J.; Cheesman, M. R.; Dooley, D. M.; Zumft, W. G. *FEBS Lett.* **1991**, *294*, 11–15.

(8) Antholine, W. A.; Kastrau, D. H. W.; Steffens, G. C. M.; Buse, G.; Zumft, W. G.; Kroneck, P. M. H. *Eur. J. Biochem.* **1992**, *209*, 875–881.

(9) Kroneck, P. M. H.; Antholine, W. A.; Riester, J.; Zumft, W. G. *FEBS Lett.* **1988**, *242*, 70–74.

(10) Neese, F.; Kappl, R.; Hüttermann, J.; Zumft, W. G.; Kroneck, P. M. H. *J. Biol. Inorg. Chem.* **1998**, *3*, 53–67.

(11) Scott, R. A.; Zumft, W. G.; Coyle, C. L.; Dooley, D. M. *Proc. Natl. Acad. Sci. U.S.A.* **1989**, *86*, 4082–4086.

(12) Dooley, D. M.; McGuirl, M. A.; Rosenzweig, A. C.; Landin, J. A.; Scott, R. A.; Zumft, W. G.; Devlin, F.; Stephens, P. J. *Inorg. Chem.* **1991**, *30*, 3006–3011.

(13) Farrar, J. A.; Neese, F.; Lappalainen, P.; Kroneck, P. M. H.; Saraste, M.; Zumft, W. G.; Thomson, A. J. *J. Am. Chem. Soc.* **1996**, *118*, 11501–11514.

(14) Dooley, D. M.; Moog, R. S.; Zumft, W. G. *J. Am. Chem. Soc.* **1987**, *109*, 6730–6735.

(15) Andrew, C. R.; Han, J.; de Vries, S.; van der Oost, J.; Averill, B. A.; Loehr, T. M.; Sanders-Loehr, J. *J. Am. Chem. Soc.* **1994**, *116*, 10805–10806.

(16) Tsukihara, T.; Aoyama, H.; Yamashita, E.; Tomizaki, T.; Yamaguchi, H.; Shinzawa-Itoh, K.; Nakashima, R.; Yaono, R.; Yoshikawa, S. *Science* **1995**, *269*, 1069–1074.

(17) Iwata, S.; Ostermeier, C.; Ludwig, B.; Michel, H. *Nature* **1995**, *376*, 660–669.

(18) Dooley, D. M.; Landin, J. A.; Rosenzweig, A. C.; Zumft, W. G.; Day, E. P. *J. Am. Chem. Soc.* **1991**, *113*, 8978–8980.

(19) Farrar, J. A.; Zumft, W. G.; Thomson, A. J. *Proc. Natl. Acad. Sci. U.S.A.* **1998**, *95*, 9891–9896.

(20) Zumft, W. G.; Dreusch, A.; Lochelt, S.; Cuypers, H.; Friedrich, B.; Schneider, B. *Eur. J. Biochem.* **1992**, *208*, 31–40.

(21) McGuirl, M. A.; Nelson, L. K.; Bollinger, J. A.; Chan, Y.-K.; Dooley, D. M. *J. Inorg. Biochem.* **1998**, *70*, 155–169.

(22) Rasmussen, T.; Berks, B. C.; Sanders-Loehr, J.; Dooley, D. M.; Zumft, W. G.; Thomson, A. J. *Biochemistry*, **2000**, *39*, 12753–12756.

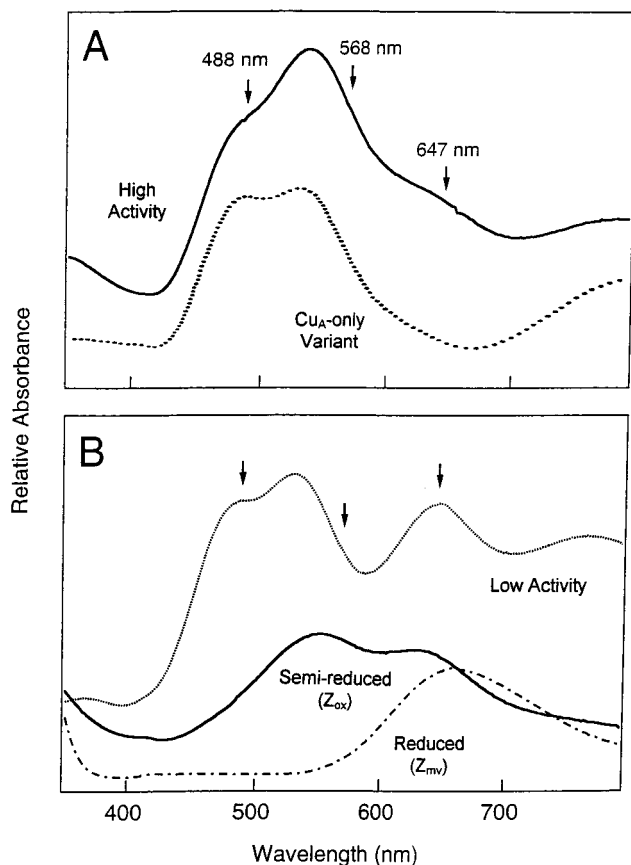


**Figure 2.** Absorption spectra of different forms of  $N_2OR$ . Arrows indicate excitation wavelengths. (A) High-activity (—) and  $Cu_A$ -only mutant (···). (B) Low-activity (···), semireduced by ascorbate (—), and reduced by dithionite (- · -).

signal at  $g = 2.02$  in the EPR spectrum of native enzyme.<sup>5,23</sup> Further support for the presence of this moiety is exhibited in the absorption spectrum of low-activity  $N_2OR$ , which, in addition to the  $Cu_A$ -assigned bands, displays a distinct transition at 650 nm (Figure 2). On the basis of the absence of this feature in the spectrum of the  $Cu_A$ -only mutant (5), as well as its correlation to low enzymatic activity,  $Z_{mv}^*$  has been ascribed to a blocked or improperly processed form of the  $Z_{ox}$  site.<sup>7</sup>

Addition of one electron-equivalent by ascorbate under anaerobic conditions produces semireduced  $N_2OR$ , in which the  $Cu_A$  site has been reduced to a spectroscopically silent  $[Cu(I) \cdot Cu(I)]$  moiety ( $A_{red}$ , Figure 1).<sup>7,24</sup> The remaining absorption bands at 550 and 640 nm (Figure 2), which are not present in the analogous spectrum of the  $Cu_A$ -only variant, have been attributed to  $Z_{ox}$ . Addition of further electron-equivalents yields the blue, reduced  $N_2OR$  (previously designated  $N_2OR$  III), with a single absorption band at 650 nm (Figure 2). This feature, which is also absent in the absorption spectrum of the reduced  $Cu_A$ -only species, has been ascribed to the reduced form of  $Z_{ox}$ , characterized as, an  $S = 1/2$  EPR-active, mixed-valence cluster ( $Z_{mv}$ , Figure 1).<sup>5</sup> Attempts to completely reduce  $Z_{mv}$  have failed, despite the addition of large excesses of a variety of reductants.<sup>5</sup>

RR spectroscopy can selectively probe Cu–S vibrations in copper–sulfur chromophores and thus provides a sensitive means of monitoring Cu–S bonding and its contribution to the overall structure of a metal site.<sup>25–27</sup> In mononuclear Cu–

cysteinate sites, excitation within the  $(Cys)S \rightarrow Cu$  ligand-to-metal charge-transfer band typically results in the enhancement of at least five vibrational fundamentals between 250 and 500  $cm^{-1}$ .<sup>26</sup> A single predominant Cu–S stretching mode,  $\nu(Cu-S)$ , can be distinguished in these spectra by its high intensity, its large frequency shift upon S or Cu isotope substitution, and its generation of high-frequency combination bands. The remaining weaker fundamentals are now attributed to modes arising from ground-state kinematic coupling of the Cu–S stretch with cysteine–ligand deformations.<sup>28–30</sup> The variations in  $\nu(Cu-S)$  frequencies among different mononuclear Cu–cysteinate sites have been proposed to serve as sensitive indicators of Cu–S bond lengths and coordination geometries, ranging from trigonal planar (430–405  $cm^{-1}$ ) to tetrahedral (405–340  $cm^{-1}$ ) to tetragonal (365–300  $cm^{-1}$ ).<sup>25</sup> Copper sites containing one cysteine and two histidine ligands in a trigonal to tetrahedral array, as in azurin and stellacyanin, compose the type 1 site of cupredoxins. Also referred to as blue copper centers due to their intense absorbance near 600 nm, these electron-transfer sites are the mononuclear counterparts to the  $Cu_A$  site.

In contrast to mononuclear copper–cysteinate sites, the dinuclear  $Cu_A$  site exhibits two distinct Cu–S stretching modes, consistent with the presence of two bridging cysteine ligands in its symmetrical  $Cu_2S_2N_2$  core.<sup>25,31,32</sup> Moreover, this center does not exhibit the continuum of coordination geometries observed for mononuclear sites but, rather, is a highly conserved, rigid structure, as evidenced by the striking consistency of the  $\nu(Cu-S)$  frequencies among native  $Cu_A$  proteins and engineered constructs.<sup>32</sup> The two  $\nu(Cu-S)$  modes experience significantly larger  $^{34}S$  isotope shifts ( $-4$  to  $-5$   $cm^{-1}$ ) than the major  $\nu(Cu-S)$  mode of mononuclear sites ( $-2$  to  $-4$   $cm^{-1}$ ). This distinction, in addition to differences in their overall  $^{34}S$  isotope-dependence patterns, reflects the relatively pure nature of the  $Cu_2S_2His_2$  vibrations and has made a normal coordinate analysis feasible. The results of these calculations<sup>31</sup> support the bridging thiolate structure and near-tetrahedral Cu coordination geometry revealed by X-ray crystal structures of  $Cu_A$  sites.<sup>4,16,17</sup>

The present RR study examines the low-energy absorption bands of all three redox states of *Pseudomonas stutzeri*  $N_2OR$  and two variants—one lacking  $Cu_A$  and the other lacking  $Cu_Z$ . Comparison of the  $Cu_A$  RR properties with those of  $Cu_A$  sites in  $CcO$ <sup>15,31,32</sup> and several engineered constructs<sup>30</sup> reveals the remarkable conservation of this rigid dinuclear copper structure, in agreement with the X-ray crystallographic findings.<sup>4</sup> Our  $^{34}S$  isotope substitution studies also address the nature of the coordination in the  $Cu_Z$  site of  $N_2OR$  and provide the strongest evidence to date that a sulfur ligand is present in  $Cu_Z$ . Whereas the RR spectra of  $Z_{ox}$  and  $Z_{mv}$  reveal a multiplicity of sulfur

(25) Andrew, C. R.; Sanders-Loehr, J. *Acc. Chem. Res.* **1996**, *29*, 365–372.

(26) Andrew, C.; Yeom, H.; Valentine, J. S.; Karlsson, B. G.; Bonander, N.; van Pouderooyen, G.; Canters, G. W.; Loehr, T. M.; Sanders-Loehr, J. *J. Am. Chem. Soc.* **1994**, *116*, 11489–11498.

(27) Dave, B. C.; Germanas, J. P.; Czernuszewicz, R. S. *J. Am. Chem. Soc.* **1993**, *115*, 12175–12176.

(28) Andrew, C. A.; Han, J.; den Blaauwen, T.; van Pouderooyen, G.; Vijgenboom, E.; Canters, G. W.; Loehr, T. M.; Sanders-Loehr, J. *J. Biol. Inorg. Chem.* **1997**, *2*, 98–107.

(29) Fraczkiewicz, R.; Fraczkiewicz, G.; Czernuszewicz, R. S., personal communication.

(30) Qiu, D.; Dasgupta, S.; Kozlowski, P. M.; Goddard, W. A., III; Spiro, T. G. *J. Am. Chem. Soc.* **1998**, *120*, 12791–12797.

(31) Andrew, C. R.; Fraczkiewicz, R.; Czernuszewicz, R. S.; Lappalainen, P.; Saraste, M.; Sanders-Loehr, J. *J. Am. Chem. Soc.* **1996**, *118*, 10436–10445.

(32) Andrew, C. A.; Lappalainen, P.; Saraste, M.; Hay, M. T.; Lu, Y.; Dennison, C.; Canters, G. W.; Fee, J. A.; Slutter, C. E.; Nakamura, N.; Sanders-Loehr, J. *J. Am. Chem. Soc.* **1995**, *117*, 10759–10760.

(23) Kroneck, P. M. H.; Riester, J.; Zumft, W. G.; Antholine, W. E. *Biol. Metals* **1990**, *3*, 103–109.

(24) Dooley, D. M.; Alvarez, M. L.; Rosenzweig, A. C.; Hollis, R. S.; Zumft, W. G. *Inorg. Chim. Acta* **1996**, *242*, 239–244.

isotope-sensitive modes, their frequencies and intensities are markedly different from one another and from those of Cu<sub>A</sub>. We propose that a single sulfide bridging up to four copper ions in Cu<sub>Z</sub>, versus two thiolates bridging two copper ions in Cu<sub>A</sub>, is responsible for the differences in the RR properties of the two mixed-valence sites (A<sub>mv</sub> and Z<sub>mv</sub>).

## Materials and Methods

Native and Cu<sub>A</sub>-only N<sub>2</sub>OR were isolated and purified as described previously<sup>5,33</sup> from *P. stutzeri* ZoBell (ATCC 14405); the latter was expressed in the mutant strain MK402, which is defective in active-site biosynthesis.<sup>5</sup> The low-activity enzyme used for these studies was purified anaerobically from cells grown under sulfur limitation and anaerobic conditions. The Z<sub>mv</sub>\* sites in this enzyme and in enzyme that has been exposed to oxygen were confirmed to be equivalent on the basis of their identical 650-nm absorption bands and RR spectra. Fully labeled [<sup>34</sup>S]N<sub>2</sub>OR was obtained from cells grown on minimal medium containing 0.25 mM Na<sub>2</sub><sup>34</sup>SO<sub>4</sub> (90 atom %, ICON). Incorporation of <sup>63</sup>Cu and <sup>65</sup>Cu (purity 99.7%) into N<sub>2</sub>OR was achieved by the *in vivo* addition of the respective isotope into a growing culture of *P. stutzeri* ZoBell, as detailed previously.<sup>6</sup> Double-labeling of N<sub>2</sub>OR with <sup>65</sup>Cu and [<sup>15</sup>N]histidine (racemic D,L-[<sup>15</sup>N α,δ1,ε2]histidine, 99% minimum <sup>15</sup>N, NIH National Stable Isotope Resource, Los Alamos, NM) was accomplished using an auxotrophic mutant generated by random transposon Tn5 mutagenesis.<sup>6,34</sup> The C622D and H583G variants were prepared and purified as described elsewhere.<sup>35</sup>

Protein samples were purified in either 25 or 50 mM Tris-HCl (pH 7.5) or 25 mM Tris-DCI (pH 7.5) buffers and were concentrated by ultrafiltration (Amicon, Microcon-50). Protein concentrations, which ranged from 0.5 to 2.5 mM protein depending on the availability of isotopic material, were determined spectrophotometrically ( $\epsilon_{280} = 114 \text{ mM}^{-1} \text{ cm}^{-1}$ ). Enzymatic activity was monitored by gas chromatography as described previously.<sup>33</sup> D<sub>2</sub>O-containing samples were prepared by diluting concentrated samples with D<sub>2</sub>O buffer and reconcentrating; the exchange was repeated at least 5 times. Aside from a 5-cm<sup>-1</sup> shift in the ice peak, no difference was observed in their RR spectra.

RR spectra were recorded on a custom McPherson 2061/207 spectrograph (0.67 m) equipped with a Princeton Instruments (LN-1100PB) liquid nitrogen-cooled CCD detector. Rayleigh scattering was attenuated using either a Kaiser Optical holographic supernotch filter or a McPherson 270 double-monochromator (600-groove grating) prefilter stage. Several lasers were used to obtain the desired excitation wavelength: Coherent Innova 302 Kr, Coherent Innova 90-6 Ar, and Coherent 599-01 dye (rhodamine 6G). Raman spectra were collected in an ~150° backscattering geometry from samples maintained at 15 K using a closed-cycle helium refrigerator (Air Products, Displex).<sup>36</sup> Air-sensitive samples were loaded and slowly frozen on the Displex in a glovebag filled with N<sub>2</sub> gas. Unless otherwise stated, spectra were obtained using an 1800-groove grating and a spectral resolution of 4 cm<sup>-1</sup>. High-quality data were generally obtained with 10-min acquisitions. Calibration of the CCD spectrometer was achieved using aspirin as a frequency standard, and absolute frequencies are accurate to ±1 cm<sup>-1</sup>. Isotope shifts, with an accuracy of ±0.5 cm<sup>-1</sup>, were obtained from spectra recorded under identical experimental conditions and were evaluated by abscissa expansion and curve resolution of overlapping bands. The programs Grams 386 (Galactic Industries) and Origin (MicroCal) were used for data analysis and data presentation, respectively.

## Results

**Raman Signature of Cu<sub>A</sub> Site.** Excitation within the 480- or 540-nm absorption bands of native N<sub>2</sub>OR yields a RR

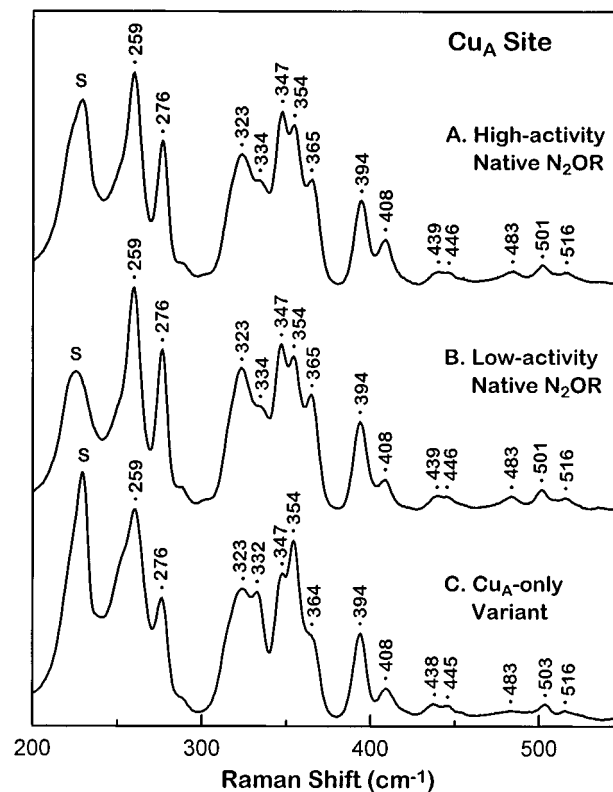


**Figure 3.** RR spectra of Cu<sub>A</sub> site (A<sub>mv</sub> cluster) obtained with 488-nm excitation. (A) High-activity N<sub>2</sub>OR (0.8 mM). (B) Low-activity N<sub>2</sub>OR (1.5 mM). (C) Cu<sub>A</sub>-only variant of N<sub>2</sub>OR (2.4 mM). S denotes 230-cm<sup>-1</sup> ice mode from frozen solvent.

spectrum (Figure 3A) closely resembling those previously reported for the Cu<sub>A</sub> sites (A<sub>mv</sub>) in N<sub>2</sub>OR from *P. stutzeri*<sup>14</sup> and *Achromobacter cycloclastes*,<sup>15</sup> cytochrome *c* oxidase (CcO),<sup>15,31,32</sup> and several engineered constructs.<sup>32</sup> The striking similarities of these spectra, as well as the spectrum obtained on the CcO Cu<sub>A</sub> site with 850-nm excitation,<sup>37</sup> have verified that all three absorption bands (i.e., at 480, 540, and 780 nm) are associated with the same copper site and that the structure of this site is conserved among the different Cu<sub>A</sub>-containing proteins. Furthermore, the presence of strongly resonance-enhanced Cu–S(Cys) stretching modes in all these spectra illustrates the substantial (Cys)S → Cu charge-transfer character of the three Cu<sub>A</sub> absorption bands.

The 488-nm excitation spectrum of native N<sub>2</sub>OR exhibits at least 11 fundamentals between 200 and 450 cm<sup>-1</sup> (Figure 3A), two of which, at 259 and 347 cm<sup>-1</sup>, are assigned as the distinctive Cu–S(Cys) stretching modes of A<sub>mv</sub> (vide infra). As reported previously,<sup>14</sup> the Raman signature of A<sub>mv</sub> in low-activity N<sub>2</sub>OR is identical to that of native high-activity enzyme (Figure 3B). Differences between high- and low-activity N<sub>2</sub>OR have been attributed to the relative contributions of Z<sub>ox</sub> and Z<sub>mv</sub>\*, which, as demonstrated by absorption spectroscopy (Figure 2), are not expected to influence A<sub>mv</sub>. In contrast, loss of the catalytic site in the Cu<sub>A</sub>-only variant does not alter the RR frequencies of A<sub>mv</sub> but causes slight changes in their relative intensities (Figure 3C). These changes, which include an increase of intensity in the 354-cm<sup>-1</sup> mode and a decrease in the features at 276, 323, 347, and 365 cm<sup>-1</sup>, are suggestive of subtle perturbations in the A<sub>mv</sub> structure. Anaerobic reduction of A<sub>mv</sub> to an EPR-silent [Cu(I)–Cu(I)] moiety occurs im-

(33) Coyle, C. L.; Zumft, W. G.; Kroneck, P. M. H.; Körner, H.; Jakob, W. *Eur. J. Biochem.* **1985**, *153*, 459–467.

(34) Zumft, W. G.; Döhler, K.; Körner, H. *J. Bacteriol.* **1985**, *163*, 918.

(35) Charnock, J. M.; Dreusch, A.; Körner, H.; Neese, F.; Nelson, J.; Kannt, A.; Michel, H.; Garner, C. D.; Kroneck, P. M. H.; Zumft, W. G. *Eur. J. Biochem.* **2000**, *267*, 1368–1381.

(36) Loehr, T.; Sanders-Loehr, J. *Methods Enzymol.* **1993**, *226*, 431–470.

(37) Wallace-Williams, S. E.; James, C. A.; de Vries, S.; Saraste, M.; Lappalainen, P.; van der Oost, J.; Fabian, M.; Palmer, G.; Woodruff, W. H. *J. Am. Chem. Soc.* **1996**, *118*, 3986–3987.

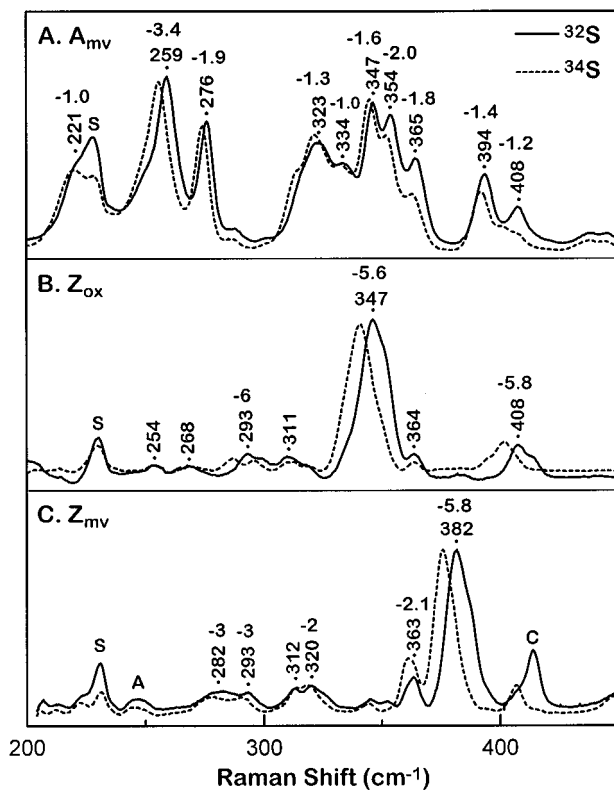


**Figure 4.** Sulfur isotope dependence of RR fundamentals. (A)  $A_{mv}$  cluster in high-activity  $N_2OR$  obtained with 488-nm excitation (2400-groove grating). (B)  $Z_{ox}$  in semireduced  $N_2OR$  probed with 568-nm excitation. (C)  $Z_{mv}$  in dithionite-reduced  $N_2OR$  probed with 647-nm excitation. Fully  $^{34}S$  labeled  $N_2OR$  was obtained from cells grown on minimal medium containing  $Na_2^{34}SO_4$ . Sample concentrations were 0.8 mM for  $[^{32}S]N_2OR$  and 1.0–1.3 mM for  $[^{34}S]N_2OR$ . Peak frequencies are listed for  $[^{32}S]$  spectra (—) with frequency shifts for the  $[^{34}S]$  spectra (---) indicated above. C denotes a band believed to arise from an altered  $Cu_A$  site (see text); its intensity is variable among preparations.

mediately upon the addition of ascorbate or dithionite to produce the semireduced and reduced forms of the enzyme, respectively. Consistent with the disappearance of the (Cys)S  $\rightarrow$  Cu charge-transfer bands at 480, 540, and 780 nm (Figure 2B), no vibrational modes attributable to  $A_{mv}$  are observed in either semireduced or reduced  $N_2OR$ .

**Isotope Dependencies of  $Cu_A$  Raman Modes.** The assignment of Cu–S(Cys) stretching vibrations can be resolved from the isotopic substitution of the coordinated cysteine sulfur atom.  $N_2OR$  is amenable to uniform  $^{34}S$  substitution by growing cells in minimal medium containing  $Na_2^{34}SO_4$  as the only sulfur source. While this preparation labels methionine residues as well as cysteine, previous studies have indicated negligible enhancement of the stretching vibrations associated with the weakly bound methionine sulfur.<sup>38,39</sup>

The two most prominent vibrational modes in the RR spectrum of  $A_{mv}$  occur at 259 and 347  $cm^{-1}$  and, upon  $^{34}S$  substitution, experience frequency shifts of  $-3.4$  and  $-1.6$   $cm^{-1}$ , respectively (Figure 4A). While several other fundamentals at 276, 354, and 365  $cm^{-1}$  exhibit substantial  $^{34}S$  isotope shifts ( $-1.9$ ,  $-2.0$ , and  $-1.8$   $cm^{-1}$ , respectively), the assignment of the 259- and 347- $cm^{-1}$  modes as the principal  $\nu(Cu-S)$  stretching vibrations is confirmed by their participation in high-

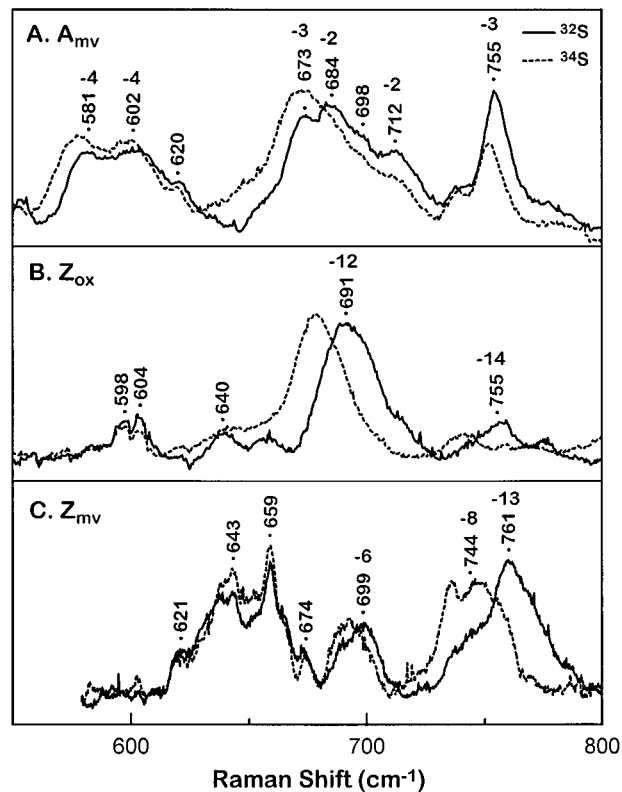


**Figure 5.** Sulfur isotope dependence of RR combination bands. (A)  $A_{mv}$  cluster in high-activity  $N_2OR$  obtained with 488-nm excitation. (B)  $Z_{ox}$  in semireduced  $N_2OR$  probed with 568-nm excitation. (C)  $Z_{mv}$  in dithionite-reduced  $N_2OR$  probed with 647-nm excitation. Sample and spectral conditions as in Figure 4.

**Table 1.** Raman Frequencies and Isotope Shifts from  $Cu_A$  ( $A_{mv}$ ) Cluster<sup>a</sup>

frequency	$\Delta^{34}S$	$\Delta^{65}Cu$	$\Delta^{15}N(His)$	assignment <sup>b</sup>
221	-1.0			
<b>259</b>	<b>-3.4</b>	<b>-0.5</b>	<b>-0.6</b>	$\nu(Cu-N)$
276	-1.9	-0.8	-1.0	
323	-1.3	0	0	
334	-1.0	0	0	
<b>347</b>	<b>-1.6</b>	<b>-0.2</b>	<b>-0.4</b>	$\nu(Cu-S)$
354	-2.0	0	-0.9	
365	-1.8	-0.3	-1.2	
394	-1.4	0	-0.4	
408	-1.2	-1.1	-0.3	
516				259 + 259
553	-2			
581	-4			259 + 323
602	-4			259 + 347
673	-3			347 + 323
684	-2			347 + 347
698				347 + 354
712	-2			347 + 365
755	-3			$\nu(S-C)$

<sup>a</sup>  $A_{mv}$  in native  $N_2OR$ . Spectra obtained with 488-nm excitation. Frequencies (in  $cm^{-1}$ ) are accurate to  $\pm 1$   $cm^{-1}$ . Boldface type indicates most intense peaks. Frequency shifts ( $\Delta$   $cm^{-1}$ ) in the presence of heavier isotopes are accurate to  $\pm 0.5$   $cm^{-1}$  for intense fundamentals and  $\pm 1.0$   $cm^{-1}$  for weak fundamentals and combination bands. <sup>b</sup> Description of major contributing vibrational modes by analogy to  $Cu_A$  site in  $CcO$ .<sup>25</sup> Assignments of combination bands are based on frequencies and S isotope dependence.

frequency combination bands (Figure 5A; Table 1). Specifically, combination bands attributable to the 259- $cm^{-1}$  fundamental are observed at 516 ( $2 \times 259$ ), 581 ( $259 + 323$ ), and 602 ( $259 + 347$ )  $cm^{-1}$ . Similarly, the 347- $cm^{-1}$  fundamental yields combination bands at 673 ( $347 + 323$ ), 684 ( $2 \times 347$ ), 698

(38) Thamann, T. J.; Willis, L. J.; Loehr, T. M. *Proc. Natl. Acad. Sci. U.S.A.* **1982**, *79*, 6396–6400.

(39) den Blaauwen, T.; Hoitink, C. W. G.; Canters, G. W.; Han, J.; Loehr, T. M.; Sanders-Loehr, J. *Biochemistry* **1993**, *32*, 12455–12464.

(347 + 354), and 712 (347 + 365)  $\text{cm}^{-1}$ . This phenomenon is reminiscent of the CcO  $\text{Cu}_A$  site, where the two  $\nu(\text{Cu-S})$  modes generate similar combination bands and have been assigned as  $A_g$  modes of the  $\text{Cu}_2\text{Cys}_2$  core.<sup>29</sup> The RR spectrum of  $\text{N}_2\text{OR}$  displays an additional vibrational mode at 755  $\text{cm}^{-1}$  (Figure 5A), which is not observed for the  $\text{Cu}_A$  site in CcO;<sup>27</sup> this S–C stretching mode is typical of mononuclear Cu–cysteinate proteins, where coupling between the Cu–S stretch and cysteine–ligand vibrations is significant.<sup>28–30</sup>

The effect of isotope substitution on the stretching vibrations of the  $\text{N}_2\text{OR}$  copper sites has also been examined using enzyme labeled with  $^{65}\text{Cu}$  and double-labeled with  $^{65}\text{Cu}$  and [ $^{15}\text{N}$ ]-histidine. On the basis of the larger mass of copper relative to sulfur, the frequency shifts upon substitution of  $^{63}\text{Cu}$  with  $^{65}\text{Cu}$  are expected to be smaller than those observed with  $^{32}\text{S}$  to  $^{34}\text{S}$  substitution. For example, while type 1 cupredoxins exhibit Cu and S isotope sensitivities in the same vibrational modes,  $^{65}\text{Cu}$  shifts are typically  $-1 \text{ cm}^{-1}$  or less compared to  $^{34}\text{S}$  shifts of  $-2$  to  $-4 \text{ cm}^{-1}$ .<sup>28,40</sup> The two  $\nu(\text{Cu-S})$  modes of the  $\text{Cu}_A$  site in  $\text{N}_2\text{OR}$  at 259 and 347  $\text{cm}^{-1}$  experience only small  $^{65}\text{Cu}$  shifts of  $-0.5$  and  $-0.2 \text{ cm}^{-1}$ , respectively, relative to their  $^{34}\text{S}$  shifts of  $-3.4$  and  $-1.6 \text{ cm}^{-1}$  (Table 1). Similar behavior has been noted in the  $\text{Cu}_A$  site of CcO, which exhibits  $^{65}\text{Cu}$  shifts of approximately  $-0.8$  and  $-1.4 \text{ cm}^{-1}$ , respectively, for the Cu–S stretching modes at 260 and 339  $\text{cm}^{-1}$ , as compared to  $^{34}\text{S}$  shifts of  $-4.1$  and  $-5.1 \text{ cm}^{-1}$  for these same fundamentals.<sup>31</sup> Only two other fundamentals of the  $\text{Cu}_A$  site in  $\text{N}_2\text{OR}$  at 276 and 365  $\text{cm}^{-1}$  undergo Cu isotope shifts. The apparent lack in  $\text{N}_2\text{OR}$  of any additional Cu isotope sensitivities in the  $\text{Cu}_A$  vibrational modes, which are expected to parallel those of S isotope dependencies, may be a consequence of the extensive coupling between the Cu–S stretching modes and the internal ligand coordinates. In this case, the corresponding  $^{65}\text{Cu}$  shifts are most likely dispersed throughout a large number of fundamentals and may lie below the detection limit.

The  $\text{Cu}_A$  modes of  $\text{N}_2\text{OR}$  are also very sensitive to [ $^{15}\text{N}$ ]-histidine substitution, with 6 of the 10 S-sensitive modes exhibiting  $^{15}\text{N}$  shifts of  $-0.4$  to  $-1.2 \text{ cm}^{-1}$  (Table 1). Whereas the small isotope shifts and lower vibrational frequencies of the [ $^{15}\text{N}$ ]histidine-sensitive modes are consistent with contributions from Cu–N(Im) vibrations, the higher energy modes, above 350  $\text{cm}^{-1}$  are not observed in type 1 copper–cysteinate sites.<sup>28,40,41</sup> Nevertheless, the extensive [ $^{15}\text{N}$ ]histidine dependence observed for the  $\text{Cu}_A$  Raman modes suggests a significant contribution from the histidine ligands.

No changes were observed in the RR spectrum of  $\text{Cu}_A$  equilibrated in  $\text{D}_2\text{O}$ , which is expected to affect both histidine and amide NH groups. However, imidazole, with only one exchangeable hydrogen, is expected to exhibit smaller deuterium shifts than the  $^{15}\text{N}$  shifts resulting from [ $^{15}\text{N}$ ]histidine substitution, and the deuterium effects may simply be too small to detect. Alternatively, a lack of deuterium shifts may reflect solvent inaccessibility of the exchangeable hydrogens. In the type 1 copper site of azurin, D shifts of  $-1$  to  $-2 \text{ cm}^{-1}$  are associated with seven vibrational modes between 372 and 476  $\text{cm}^{-1}$  and are ascribed to the amide NH of cysteine and adjacent residues.<sup>28</sup> The failure to observe this type of D-dependence in  $A_{mv}$  or  $\text{N}_2\text{OR}$  suggests that the coupling of ligand vibrations does not extend as far into the polypeptide backbone.

**Raman Signature of the  $Z_{ox}$  Site.** The absorption bands at 550 and 640 nm that remain following the reduction of  $A_{mv}$

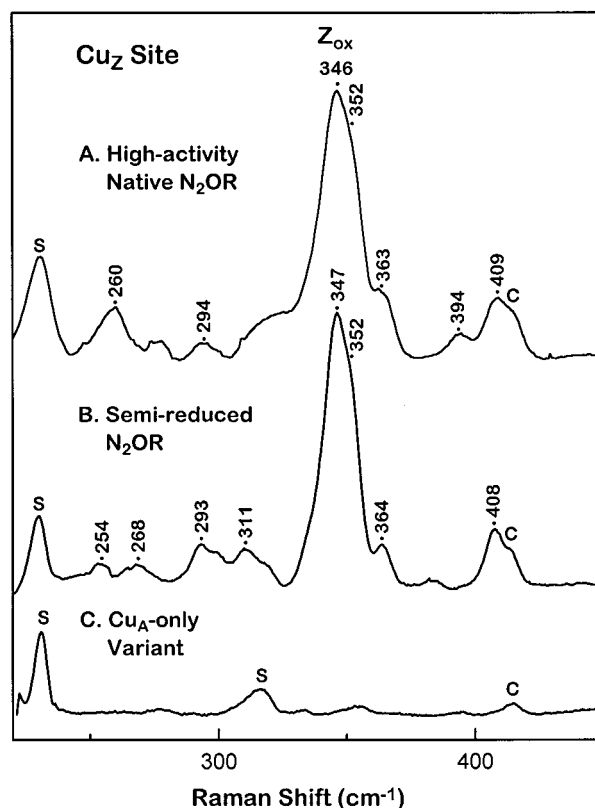


**Figure 6.** RR spectra of  $\text{Cu}_Z$  site ( $Z_{ox}$  cluster) obtained with 568-nm excitation. (A)  $Z_{ox}$  in high-activity  $\text{N}_2\text{OR}$  (0.8 mM). (B)  $Z_{ox}$  in  $\text{N}_2\text{OR}$  (0.8 mM) semireduced by ascorbate. (C)  $\text{Cu}_A$ -only variant of  $\text{N}_2\text{OR}$  (2.4 mM) probed with 578-nm excitation. C denotes 414- $\text{cm}^{-1}$  peak from an altered- $\text{Cu}_A$  contaminant (see text).

with ascorbate (Figure 2B, semireduced) have previously been attributed to an antiferromagnetically coupled  $[\text{Cu(II)}\cdot\text{Cu(II)}]$  moiety, previously referred to as  $Z_{ox}$ .<sup>7,24</sup> On the basis of the crystallographic results,  $Z_{ox}$  may be formulated as an antiferromagnetically coupled Cu(II) tetramer or perhaps as a  $[\text{Cu(II)}\cdot\text{Cu(II)}]$  dimer with a neighboring  $[\text{Cu(I)}\cdot\text{Cu(I)}]$  dimer. In either case, bridging ligands among the Cu(II) ions would be required to mediate the magnetic coupling. Excitation within the 550-nm band yields a RR spectrum dominated by a single vibrational mode at 347  $\text{cm}^{-1}$ , with several weaker features in the 200–450- $\text{cm}^{-1}$  region (Figure 6B). The analogous RR spectrum of native  $\text{N}_2\text{OR}$  with 568-nm excitation is close to that of the semireduced enzyme in terms of both frequencies and intensities (Figure 6A), demonstrating that  $A_{mv}$  does not contribute to the 568-nm excitation spectrum and that its reduction does not affect  $Z_{ox}$ , which is expected given the separation between these centers observed in the crystal structure.

The variant  $\text{N}_2\text{OR}$ , which lacks the  $\text{Cu}_Z$  site, does not exhibit the Raman signature of  $Z_{ox}$  (Figure 6C), but displays a single fundamental at 414  $\text{cm}^{-1}$  (labeled C), which is also present in the RR spectra of native, semireduced, and reduced enzyme, and displays an excitation maximum near 620 nm. The variable intensity of this mode in different sample preparations suggests that the contribution of this site is dependent on isolation conditions. On the basis of its continued presence after reduction with ascorbate or dithionite (Figure 7B and D), as well as its S isotope shift of  $-7 \text{ cm}^{-1}$  (Figure 4C), this copper–sulfur vibration is assigned to an altered Cu site. The Cu–S species responsible for the 414- $\text{cm}^{-1}$  feature most likely derives from modification of a  $\text{Cu}_A$  site because it is observed in the  $\text{Cu}_A$ -

(40) Qiu, D.; Dong, S.; Ybe, J. A.; Hecht, M. H.; Spiro, T. G. *J. Am. Chem. Soc.* **1995**, *117*, 6443–6446.

(41) Sanders-Loehr, J. In *Bioinorganic Chemistry of Copper*; Karlin, K. D., Tyecklár, Z., Eds.; Chapman Hall: New York, 1993; pp 51–63.

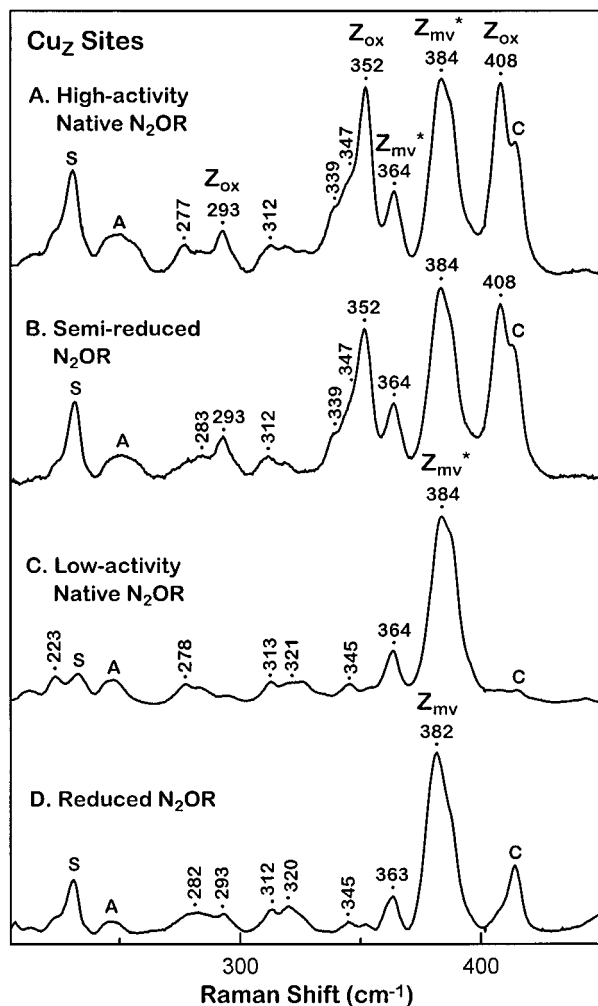


**Figure 7.** RR spectra of  $\text{Cu}_2$  sites obtained with 647-nm excitation. (A) Mixture of  $Z_{\text{ox}}$  and  $Z_{\text{mv}}^*$  in high-activity  $\text{N}_2\text{OR}$ ; samples as in Figures 3A and 6A. (B) Mixture of  $Z_{\text{ox}}$  and  $Z_{\text{mv}}^*$  in semireduced  $\text{N}_2\text{OR}$ ; sample as in Figure 6B. (C)  $Z_{\text{mv}}^*$  in low-activity  $\text{N}_2\text{OR}$ ; sample as in Figure 3B. (D)  $Z_{\text{mv}}$  in dithionite-reduced  $\text{N}_2\text{OR}$  (0.8 mM). A denotes artifact attributable to 647-nm notch filter.

only variant (Figure 6C) but not in the  $\text{Cu}_2$ -only variant (the C622D mutant, described below).

Excitation within the 640-nm band of native or semireduced  $\text{N}_2\text{OR}$  (Figure 7A and B, respectively) yields the same set of Raman frequencies at 347, 352, and 408  $\text{cm}^{-1}$  that were attributed to  $Z_{\text{ox}}$  in the 568-nm excitation spectrum and thus establishes a common copper–sulfide ground-state structure for both absorption bands. However, the relative intensities of these fundamentals differ significantly at the two excitation wavelengths, indicating that the corresponding absorption bands must be associated with different excited-state structures, i.e., different electronic transitions. Specifically, when samples are excited at 647 nm, the 347- $\text{cm}^{-1}$  fundamental loses intensity while that of the 352- and 408- $\text{cm}^{-1}$  features are greatly enhanced. Further complexity in the interpretation of the 647-nm excitation spectrum arises from the presence of a second copper–sulfide species with features at 364 and 384  $\text{cm}^{-1}$ ; this species has been assigned to  $Z_{\text{mv}}^*$ , a catalytically inactive variant of  $Z_{\text{ox}}$  (vide infra).

**Isotope Dependencies of the  $Z_{\text{ox}}$  Raman Modes.** An unusual feature of the RR spectrum obtained with 568-nm excitation is that three of the fundamentals at 293, 347, and 408  $\text{cm}^{-1}$  have substantial Cu–S stretching character, as evidenced by their

**Table 2.** Raman Frequencies and Isotope Shifts from  $Z_{\text{ox}}$  Cluster<sup>a</sup>

frequency	$\Delta^{34}\text{S}$	$\Delta^{65}\text{Cu}$	$\Delta^{15}\text{N}(\text{His})$	assignment
254	0			
268	0			
293	-6	-1	0	$\nu(\text{Cu}-\text{S})$
311	0	-1	0	
347	-5.6	-1.9	0	$\nu(\text{Cu}-\text{S})$
352 <sup>b</sup>	-2.5	-1.2	-0.6	
364	0			
408 <sup>b</sup>	-5.8	-1.8	-0.3	$\nu(\text{Cu}-\text{S})$
640 <sup>b</sup>	-5	-2	0	352 + 293
691	-12	-4	0	347 + 347
700 <sup>b</sup>	-4	-3	-1	352 + 352
755	-14	-5	0	347 + 408
759 <sup>b</sup>	-10	-3	-1	352 + 408

<sup>a</sup> $Z_{\text{ox}}$  site in semireduced  $\text{N}_2\text{OR}$ . Spectra obtained with excitation at 568 (S isotopes) or 578 nm (Cu and N isotopes). Frequencies and assignments as in Table 1. Identification of  $\nu(\text{Cu}-\text{S})$  are based on S isotope shifts. <sup>b</sup>Data obtained with 647-nm excitation.

large S isotope shifts of -6.0, -5.6, and -5.8  $\text{cm}^{-1}$ , respectively (Figure 4B). The atypical RR signature of  $Z_{\text{ox}}$  identifies this metal site as a novel copper–sulfide species, containing Cu(II) and  $\text{S}^{2-}$ , where the sulfide ligand bridges at least two Cu(II) ions. The attribution of three major Cu–S stretching modes to a single Cu(II)–sulfide chromophore is supported by their resonance enhancement upon excitation within both  $\text{S}^{2-} \rightarrow \text{Cu}$  charge-transfer transitions, at 550 and 650 nm (Figures 6A and 7A,B), and by their involvement in combination bands (Figure 5B; Table 2). For example, 568-nm excitation produces combination bands at 691 ( $2 \times 347$ ) and 755 ( $347 + 408$ )  $\text{cm}^{-1}$ , with respective S isotope shifts of -12 and -14  $\text{cm}^{-1}$ , and 647-nm excitation yields combination bands at 640 ( $352 + 293$ ), 700 ( $2 \times 352$ ), and 759 ( $352 + 408$ )  $\text{cm}^{-1}$ , with respective S isotope shifts of -5, -4, and -10  $\text{cm}^{-1}$ . The behavior of the 293- and 352- $\text{cm}^{-1}$  fundamentals is also unusual. Despite a large S isotope shift of -6.0  $\text{cm}^{-1}$ , the intensity of the 293- $\text{cm}^{-1}$  mode is relatively weak in both the 568- and 647-nm excitation spectra and contributes to only one combination band at 640  $\text{cm}^{-1}$ . Conversely, the 352- $\text{cm}^{-1}$  mode is intense in both spectra yet experiences a smaller S isotope shift of -2.5  $\text{cm}^{-1}$ , suggesting that this vibration has less Cu–S stretching character. Nevertheless, this fundamental generates several combination bands, including an overtone at 700 ( $2 \times 352$ )  $\text{cm}^{-1}$  and the combination band with the 293- $\text{cm}^{-1}$  mode.

The isotope shifts displayed by the RR modes of  $Z_{\text{ox}}$  upon <sup>65</sup>Cu substitution, although smaller in magnitude, parallel those resulting from <sup>34</sup>S substitution (Table 2). In addition, [<sup>15</sup>N]-histidine substitution has almost no effect on the RR spectrum, suggesting only minor kinematic coupling between Cu–imidazole stretching modes and the Cu– $\text{S}^{2-}$  chromophore. These results, which imply that the Cu isotope shifts originate mainly from Cu–S rather than Cu–N(Im) vibrations, are consistent with the weak intensity of the low-frequency Cu–N(Im) fundamentals (<290  $\text{cm}^{-1}$ , which are only weakly enhanced), and the fairly pure nature of the Cu–S stretching modes at 293, 347, and 408  $\text{cm}^{-1}$ .

**Raman Signature of the  $Z_{\text{mv}}$  Site.** Treatment of native  $\text{N}_2\text{OR}$  with dithionite results in the conversion of  $A_{\text{mv}}$  to  $A_{\text{red}}$  and  $Z_{\text{ox}}$  to  $Z_{\text{mv}}$  and the appearance of a new absorption band at 650 nm characteristic of  $Z_{\text{mv}}$  (Figure 2B, reduced). Excitation of dithionite-reduced  $\text{N}_2\text{OR}$  at 647 nm produces a new RR spectrum with a dominant vibrational mode at 382  $\text{cm}^{-1}$  (Figure 7D), proving that  $Z_{\text{mv}}$  has a distinctly different copper–sulfide ground-state structure from  $Z_{\text{ox}}$ , whose dominant vibrational modes are at 352 and 408  $\text{cm}^{-1}$  with this excitation wavelength (Figure 7A,B). The 647-nm spectral pattern for  $Z_{\text{mv}}$  is somewhat

**Table 3.** Raman Frequencies and Isotope Shifts from Reduced Cu<sub>Z</sub> Sites<sup>a</sup>

$Z_{mv}$					$Z_{mv}^*$				
freq	$\Delta^{34}\text{S}$	$\Delta^{65}\text{Cu}$	$\Delta^{15}\text{N}(\text{His})$	assignment	freq	$\Delta^{34}\text{S}$	$\Delta^{65}\text{Cu}$	$\Delta^{15}\text{N}(\text{His})$	assignment
282	-3	0	0		278				
293	-3	-1	0		294				
312	0	0	0		313				
320	-2	-2	-1		321				
345	-1	0	0		345				
363	-2.1	-0.6	-0.6		364	-1.0	-0.4	-1.2	
<b>382</b>	<b>-5.8</b>	<b>-0.8</b>	<b>0</b>	$\nu(\text{Cu-S})$	<b>384</b>	<b>-4.7</b>	<b>-2.0</b>	<b>-0.6</b>	$\nu(\text{Cu-S})$
699	-6			382 + 320	701	-6			384 + 321
744	-8			382 + 363	747	-6			384 + 364
761	-13			382 + 382	766	-9			384 + 384

<sup>a</sup>  $Z_{mv}$  cluster from reduced N<sub>2</sub>OR.  $Z_{mv}^*$  cluster from low-activity N<sub>2</sub>OR (frequencies) and high-activity N<sub>2</sub>OR (isotope shifts). Spectra obtained with 647-nm excitation. Frequencies and assignments as in Tables 1 and 2.

similar to that of  $Z_{ox}$  (568-nm excitation) in that a single intense feature is observed at 382 (Figure 7D) and 347 cm<sup>-1</sup> (Figure 6A), respectively, each with a high-frequency shoulder and a number of weaker features, primarily to lower frequencies. Although RR data were not collected on the reduced Cu<sub>A</sub>-only mutant, previous work has verified that this form of the enzyme has no significant absorbance in the 400–800-nm region, consistent with the reduction of the Cu<sub>A</sub> site and the absence of the Cu<sub>Z</sub> site.<sup>5</sup>

**Isotope Dependencies of the  $Z_{mv}$  Raman Modes.** The sulfur isotope dependence of the  $Z_{mv}$  site is again similar to the  $Z_{ox}$  site in that the most intense feature at 382 cm<sup>-1</sup> exhibits the largest <sup>34</sup>S shift of -5.8 cm<sup>-1</sup> (Figure 4C). Smaller shifts of -2 to -3 cm<sup>-1</sup> are seen in a number of the lower intensity modes. These assessments are confirmed by the appearance of three <sup>34</sup>S-sensitive combination bands at 699 (382 + 320), 744 (382 + 363), and 761 (2 × 382) cm<sup>-1</sup>, with respective S isotope shifts of -6, -8, and -13 cm<sup>-1</sup> (Figure 5C; Table 3). The role of the major  $\nu(\text{Cu-S})$  stretching mode as the generator of these combination bands is similar to the behavior observed for thiolate ligation, as illustrated by type 1 cupredoxins.<sup>26</sup> The RR modes of  $Z_{mv}$  experience <sup>65</sup>Cu and [<sup>15</sup>N]histidine isotope sensitivities similar to those of  $Z_{ox}$ , in that <sup>65</sup>Cu shifts correlate well with those produced by <sup>34</sup>S substitution and almost no effect is observed upon [<sup>15</sup>N]histidine substitution (Table 3). This finding suggests that, in contrast to the Cu<sub>A</sub> site, the contribution of histidine ligands to the RR properties of the Cu<sub>Z</sub> site is minor, regardless of its oxidation state. This is an interesting finding that warrants further investigation in light of the multiple histidine ligands in the Cu<sub>Z</sub> cluster.

**Raman Signature of the  $Z_{mv}^*$  Site.** The loss of enzymatic activity upon aerobic isolation and purification of N<sub>2</sub>OR has previously been correlated to the amount of  $Z_{mv}^*$ ,<sup>5,33</sup> a mixed-valence form of the Cu<sub>Z</sub> site whose presence, like that of  $Z_{mv}$ , is manifested as an absorption band at 650 nm (Figure 2). Excitation within this band yields a RR spectrum for  $Z_{mv}^*$  (Figure 7C) that is remarkably similar to that of  $Z_{mv}$  (Figure 7D) in terms of fundamental frequencies, combination bands, and S isotope shifts (Table 3). Nevertheless, a distinction of 2 cm<sup>-1</sup> is clearly evident in their dominant Cu-S stretching modes, i.e., 384 cm<sup>-1</sup> in  $Z_{mv}^*$  versus 382 cm<sup>-1</sup> in  $Z_{mv}$ , perhaps indicating a minor structural difference, such as variation in the number or coordination of the solvent-derived ligands apparent in the structure.

As predicted from absorption, EPR, and MCD spectroscopy,<sup>5,7,33</sup> the contribution of  $Z_{mv}^*$  to the 647-nm excitation spectrum of high-activity N<sub>2</sub>OR is dramatically smaller (relative to the solvent peak, S) than that of low-activity enzyme, (Figure 7A and C, respectively). No changes are seen in the RR

spectrum upon the addition of ascorbate to high-activity enzyme (Figure 7B), indicating that neither  $Z_{ox}$  nor  $Z_{mv}^*$  is reduced by this reagent. This is apparently inconsistent with the observation by Farrar et al. that  $Z_{mv}^*$ , like  $A_{mv}$ , can be reduced by ascorbate to an EPR-silent moiety.<sup>7</sup> Although these differences may simply reflect a slower reduction of  $Z_{mv}^*$  compared to  $A_{mv}$ , attempts to reduce  $Z_{mv}^*$  in low-activity N<sub>2</sub>OR by addition of dithionite in this laboratory have also failed, as evidenced by a lack of change in the RR and absorption spectra (data not shown).

**Raman Spectra of Copper Site Variants.** Recently two variants of N<sub>2</sub>OR were prepared and purified: C622D, in which one of the strictly conserved Cu<sub>A</sub> cysteine ligands has been changed; and H583G, in which one of the Cu<sub>A</sub> histidine ligands has been mutated.<sup>35</sup> Excitation at 488 nm reveals that a slightly perturbed Cu<sub>A</sub> site is present in H583G but that Cu<sub>A</sub> is absent in C622D, as expected (Figure 8A). These results clearly illustrate the critical importance of both cysteines in the assembly of the Cu<sub>A</sub> center and the robustness of its Cu<sub>2</sub>S<sub>2</sub> core. The RR frequencies of the Cu<sub>A</sub> site in H583G are closely similar to those of the wild-type enzyme (Figure 3A), except for the lower frequency features at 265 and 275 cm<sup>-1</sup>, which are shifted slightly and are somewhat less intense. These changes are consistent with greater Cu-histidine vibrational contributions in the low-frequency region (Table 1) and suggest that the loss or replacement of a histidine ligand does not perturb the remainder of the Cu<sub>2</sub>S<sub>2</sub> core. A remarkably different picture emerges from the spectra collected with 647-nm excitation (Figure 8B). Notably, the RR spectrum of C622D is essentially identical to that of  $Z_{mv}^*$  (Figure 7C), thereby providing strong support for the assignment of the absorption band and RR features to the Cu<sub>Z</sub> site. Note that there is essentially no indication of a  $Z_{ox}$  center in the C622D spectrum (Figure 8B), whereas features attributable to both  $Z_{mv}^*$  and  $Z_{ox}$  are evident in the spectrum of H583G. This suggests that the proper folding of the protein around the Cu<sub>A</sub> site can influence the structure or redox properties (or both) of the Cu<sub>Z</sub> site.

## Discussion

**Structure of the Cu<sub>A</sub> Site.** The Raman spectra of Cu<sub>A</sub> in N<sub>2</sub>OR from *P. stutzeri* (Figure 3A) and *A. cycloclastes*<sup>15</sup> are nearly identical in terms of the Cu-S stretching frequencies, their relative intensities, and the total number of fundamentals in the 200–450-cm<sup>-1</sup> region. As previously noted,<sup>25</sup> the remarkable consistency of  $\pm 4$  cm<sup>-1</sup> for the two  $\nu(\text{Cu-S})$  modes at 260 and 343 cm<sup>-1</sup> in all known Cu<sub>A</sub>-containing moieties reflects the rigidity of this site imparted by the two bridging thiolates and is sharply contrasted by that of the single  $\nu(\text{Cu-S})$  mode near 390 cm<sup>-1</sup> in mononuclear type I Cu-cysteinate sites, which can vary by as much as  $\pm 38$  cm<sup>-1</sup>. At the current



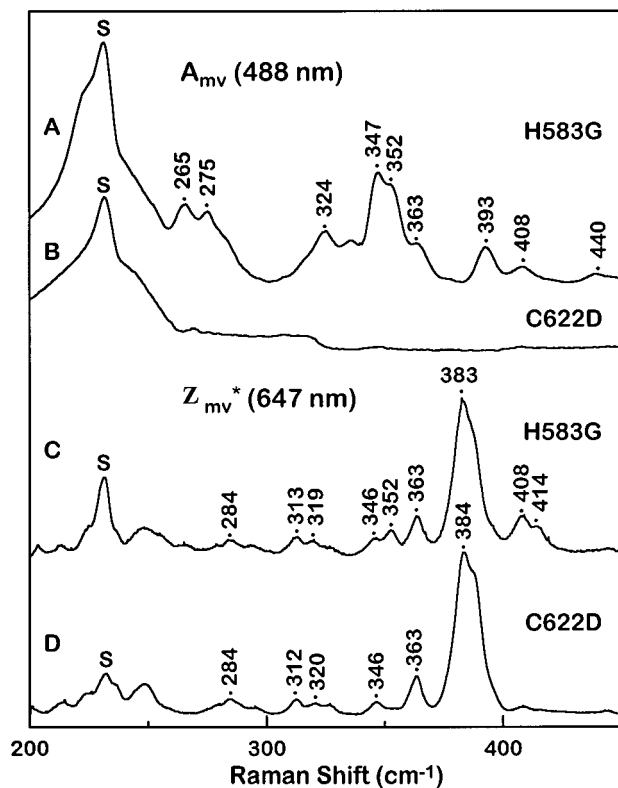


**Figure 8.** Resonance Raman spectra of H583G and C622D site-directed mutants of N<sub>2</sub>OR. (A) A<sub>mv</sub> in H583G N<sub>2</sub>OR (0.7 mM) probed with 488-nm excitation. (B) A<sub>mv</sub> in C622D N<sub>2</sub>OR (1.2 mM) probed with 488-nm excitation. (C) and (D), Z<sub>mv</sub>\* sites in H583G and C622D, respectively, probed with 647-nm excitation.

resolution of the structures for CcO and N<sub>2</sub>OR, the Cu<sub>A</sub> sites in these two enzymes are practically identical. Minor structural variability in the Cu<sub>A</sub> sites from N<sub>2</sub>OR and CcO are detectable by RR spectroscopy and are manifested in the number of weaker fundamentals between 200 and 450 cm<sup>-1</sup> and their distinctive <sup>34</sup>S dependence patterns (Figure 9A). The Cu<sub>A</sub> spectra of CcO fragments from several sources reveal three well-resolved RR modes in this region, three of which are S isotope dependent and two of which are N isotope dependent.<sup>31,32</sup> A normal coordinate analysis (NCA) reveals that the RR spectrum of the Cu<sub>A</sub> site in *Paracoccus denitrificans* CcO can be described as a set of coupled Cu–S and Cu–N vibrations arising from the Cu<sub>2</sub>S<sub>2</sub> core and two terminal imidazoles with very little contribution from the cysteine ligand side chain.<sup>31</sup> In contrast, the RR spectrum of N<sub>2</sub>OR Cu<sub>A</sub> (Figure 9A) contains a much larger number of vibrational modes and more closely resembles that of the Cu<sub>A</sub> construct from amicyanin,<sup>32</sup> a blue copper protein that has been converted to a Cu<sub>A</sub> site by the addition of a cysteine-containing Cu-binding loop.<sup>42</sup> The observation of nine fundamentals in the Cu<sub>A</sub> spectrum of N<sub>2</sub>OR, all of which are S isotope sensitive, and seven of which are N isotope sensitive, suggests a greater degree of coordinate mixing of internal cysteine–ligand vibrations with Cu–S and Cu–N stretching. In addition, a cysteine–ligand S–C stretch is observed at 755 cm<sup>-1</sup> in the RR spectrum of N<sub>2</sub>OR (Figure 5A) but not in that of CcO. The presence of this mode, which is typical of mononuclear Cu–cysteine proteins, where coupling between the Cu–S stretching mode and cysteine–ligand vibrations is significant,<sup>24</sup> further illustrates the extensive kinematic coupling present in the Cu<sub>A</sub> site of N<sub>2</sub>OR.

(42) Dennison, C.; Vijgenboom, E.; de Vries, S.; van der Oost, J.; Canters, G. W. *FEBS Lett.* **1995**, *365*, 92–94.

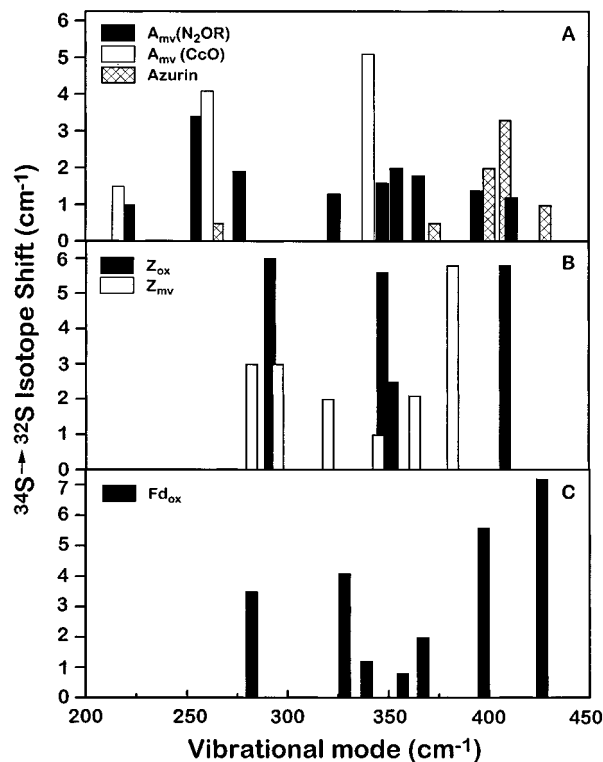


**Figure 9.** Sulfur isotope dependence of individual RR modes. (A) Cu<sub>A</sub> site in N<sub>2</sub>OR from *P. stutzeri* (data from Figure 4A); Cu<sub>A</sub> site in CcO fragment from *P. denitrificans* (data from ref 25); and type 1 site in azurin from *Pseudomonas aeruginosa* (data from ref 41). (B) Z<sub>ox</sub> in semireduced N<sub>2</sub>OR (data from Figure 4B) and Z<sub>mv</sub> in dithionite-reduced N<sub>2</sub>OR (data from Figure 4C). (C) Fe<sub>2</sub>S<sub>2</sub>(Cys)<sub>4</sub> site in ferredoxin from *Prophyra umbilicalis* (data from ref 56).

**Table 4.** Calculated and Observed Isotope Shifts for Copper–S(Cys) Sites<sup>a</sup>

species	Cu– <sup>34</sup> S	<sup>65</sup> Cu–(S,N)	Cu– <sup>15</sup> N(His)
calculated shifts (sum)			
CuL <sup>b</sup>	–7.9	–5.3	–2.8
CuSCu, (ν <sub>s</sub> + ν <sub>as</sub> ) <sup>c</sup>	–13.0		
Cu <sub>2</sub> S <sub>2</sub> (Im) <sub>2</sub> , A <sub>g</sub> modes <sup>d</sup>	–8.7	–4.8	–1.8
Cu <sub>2</sub> S <sub>2</sub> (Im) <sub>2</sub> , all modes <sup>d</sup>	–29.3	–13.1	–4.5
observed shifts (sum)			
CuS(His) <sub>2</sub> in azurin <sup>e</sup>	–7.5	–2.4	–1.0
Cu <sub>A</sub> (A <sub>mv</sub> ) in CcO <sup>f</sup>	–10.7	–3.8	–2.0
Cu <sub>A</sub> (A <sub>mv</sub> ) in native N <sub>2</sub> OR <sup>g</sup>	–16.6	–1.8	–4.5
Z <sub>ox</sub> in native N <sub>2</sub> OR <sup>g</sup>	–19.9	–6.9	–0.9
Z <sub>mv</sub> in reduced N <sub>2</sub> OR <sup>g</sup>	–16.9	–4.4	–1.6

<sup>a</sup> Sum of isotope shifts in all fundamentals between 210 and 450 cm<sup>-1</sup>. Downshifts relative to frequencies for <sup>32</sup>S, <sup>14</sup>N, or <sup>65</sup>Cu.

<sup>b</sup> Calculated for a diatomic oscillator with a copper–ligand (CuL) vibration at 400 cm<sup>-1</sup>. Imidazole is treated as a point mass of 68 (<sup>14</sup>N) or 70 (<sup>15</sup>N). <sup>c</sup> Sum of shifts for ν<sub>s</sub>(Cu–S–Cu) and ν<sub>as</sub>(Cu–S–Cu) in a singly bridged cluster, calculated according to ref 39. <sup>d</sup> Sum of calculated shifts for CuL coordinates in a di-μ-S-bridged cluster with two terminal imidazoles (treated as point masses of 68). Based on NCA calculations in ref 25. <sup>e</sup> Azurin from *Pseudomonas aeruginosa*. Sum of <sup>34</sup>S shifts, based on curve-fitting, from ref 41 and Figure 8. <sup>f</sup> Sum of <sup>15</sup>N and <sup>65</sup>Cu shifts for H117G mutant plus exogenous imidazole from ref 35. <sup>g</sup> Sum of isotope shifts for Cu<sub>A</sub>-containing fragment in *P. denitrificans* CcO from ref 25. <sup>h</sup> Sum of isotope shifts for Cu<sub>A</sub>, Z<sub>ox</sub>, and Z<sub>mv</sub> in *P. stutzeri* N<sub>2</sub>OR from Tables 1–3, respectively.

Increased coupling in the Cu<sub>A</sub> site of N<sub>2</sub>OR is also evident in the comparison of their total S isotope shifts (Table 4). The total S isotope shift of the three S-sensitive fundamentals of *P. denitrificans* CcO Cu<sub>A</sub> is –10.7 cm<sup>-1</sup> (Table 4). These isotope shifts, as well as the large 79-cm<sup>-1</sup> energy separation between the two predominant S-sensitive modes at 260 and 339 cm<sup>-1</sup>,

**Table 5.** Spectral Characteristics of Cu<sub>A</sub> and Cu<sub>Z</sub> Sites in N<sub>2</sub>OR

property	A <sub>mv</sub>	Z <sub>ox</sub>	Z <sub>mv</sub> (Z <sub>mv</sub> <sup>*</sup> )
Cu valence <sup>a</sup>	+1.5, +1.5	+2, +2	+1.5, +1.5
absorption max (nm)	480, 540, 780	550, 640	650
magnetic properties	S = 1/2	S = 0	S = 1/2
EPR, A <sub>  </sub>	7-line <sup>b</sup>	none	
MCD (nm) <sup>c</sup>	−473, +525, −750	none	+625, −680,
ν(Cu–S) (cm <sup>−1</sup> ) <sup>d</sup>			
488-nm excitation	<b>259, 276, 347,</b> 354		
568-nm excitation		293, <b>347, 352,</b> 408	
647-nm excitation		293, 347, <b>352,</b> <b>408</b>	363, <b>382</b>
sum of Δ <sup>34</sup> S <sup>e</sup>	−17 (±5)	−20 (±2)	−17 (±4)

<sup>a</sup> For the two copper ions in the Cu<sub>A</sub> site and two of the four ions in the Cu<sub>Z</sub> site. <sup>b</sup>Reference 8. <sup>c</sup>Reference 6. <sup>d</sup>This work. Identification of Cu–S stretching modes as in Tables 1–3. Boldface type denotes most intense Raman features. <sup>e</sup>Table 4.

have been fitted to a dinuclear copper model containing two bridging thiolates and two imidazoles trans-distorted from the Cu<sub>2</sub>S<sub>2</sub> plane.<sup>31</sup> On the basis of these NCA calculations, three symmetric A<sub>g</sub> modes are assigned to the Cu<sub>A</sub> site: the 339-cm<sup>−1</sup> mode is the totally symmetric stretch of the Cu<sub>2</sub>S<sub>2</sub> rhombus; the 260-cm<sup>−1</sup> mode has contributions from both Cu–S and Cu–N(Im) stretching modes; and a 138-cm<sup>−1</sup> mode accounts for the motion of the two Cu atoms along the Cu–Cu axis, whose origin as either a Cu–S–Cu bend or a Cu–Cu stretch remains unclear.<sup>31,43</sup> The Cu<sub>A</sub> site in N<sub>2</sub>OR also displays a large energy separation between the two ν(Cu–S) modes of 88 cm<sup>−1</sup>, but the S isotope pattern, with 10 S-sensitive modes, is significantly different (Figure 9A). While still consistent with the NCA for a Cu<sub>A</sub>-type site, the larger total S isotope shift of −16.6 cm<sup>−1</sup> and the increased number of S-sensitive modes suggest the participation of more than only A<sub>g</sub> modes (Table 4). Such behavior most likely implies greater coupling of the Cu–S stretches with vibrations of the two cysteine backbones. Nevertheless, the RR spectroscopic data for A<sub>mv</sub> in N<sub>2</sub>OR strongly support a dithiolate-bridged cluster geometry as observed in the crystal structures of reduced N<sub>2</sub>OR (where Cu<sub>A</sub> is present as the [Cu(I)•Cu(I)] dimer) and of CcO (Table 5).

It is of interest that the Cu<sub>A</sub> site in N<sub>2</sub>OR also exhibits more vibrational coupling of the Cu–N(His) modes with the Cu–S(Cys) stretch, as evidenced by the larger total [<sup>15</sup>N]histidine shift of −4.5 cm<sup>−1</sup>, relative to −2.0 cm<sup>−1</sup> in CcO (Table 4). Although this type of [<sup>15</sup>N]His dependence is not observed in mononuclear Cu(Cys)(His)<sub>2</sub> sites,<sup>37</sup> a comparable total [<sup>15</sup>N]-histidine shift of −4.3 cm<sup>−1</sup> is observed for the dinuclear iron site in Rieske ferredoxins when the two histidine imidazoles of the (Cys)<sub>2</sub>FeS<sub>2</sub>Fe(His)<sub>2</sub> cluster are double-labeled with <sup>15</sup>N.<sup>44</sup> In addition, N-sensitive iron–sulfur modes are found between 320 and 360 cm<sup>−1</sup>, due to coupling of the metal–imidazole and metal–sulfur stretches, as in N<sub>2</sub>OR Cu<sub>A</sub>. Evidently, this coordinate mixing does not require coplanarity because the two terminal histidines of Rieske proteins are tetrahedrally coordinated to one iron, and the imidazole rings are not coplanar with the Fe<sub>2</sub>S<sub>2</sub> core. Precedence for the enhancement of metal–N(His) vibrations at higher vibrational frequencies is also found in oxyhemocyanin, a dicopper site with six histidine ligands, which displays six imidazole-dependent RR modes between 220

(43) Wallace-Williams, S. E.; James, C. A.; de Vries, S.; Saraste, M.; Lappalainen, P.; van der Oost, J.; Fabian, M.; Palmer, G.; Woodruff, W. H. *J. Am. Chem. Soc.* **1996**, *118*, 3986–3987.

(44) Rotsaert, F. A. J.; Pikus, J. D.; Fox, B. G.; Markley, J. L.; Sanders-Loehr, J., unpublished results.

and 345 cm<sup>−1</sup> upon excitation within its peroxide → Cu(II) CT band.<sup>45</sup> In this case, the copper atoms are bridged by a side-on bound (μ-η<sup>2</sup>:η<sup>2</sup>) peroxide, which allows coupling of Cu–N(His) and Cu–O(peroxide) stretches. Thus, it appears that histidine ligand modes are more likely to undergo coordinate mixing in sites where the metals are rigidly positioned by multiple bridging ligands, as in Cu<sub>A</sub>, Rieske ferredoxins, and oxyhemocyanin or by heme groups as in myoglobin.<sup>46</sup>

**Structure of the Z<sub>ox</sub> Site.** It is clear from the crystal structure that there are no thiolate ligands in the Cu<sub>Z</sub> site, as predicted from the sequence analysis. As pointed out above, the RR spectrum of the Z<sub>ox</sub> site in high-activity or semireduced N<sub>2</sub>OR exhibits four sulfur isotope-sensitive modes at 293, 347, 352, and 408 cm<sup>−1</sup> whose intensity is dependent on excitation wavelength (Figures 6A and 7A). Consequently, there must be a sulfur ligand present that is capable of generating low-energy charge-transfer transitions. The pattern of <sup>34</sup>S shifts in Z<sub>ox</sub> is completely different from that in mononuclear cupredoxins such as azurin. The Cu–S stretch in azurin is coupled with cysteine ligand vibrations of *similar* energy such that most of the isotope-sensitive modes are found in a narrow frequency range of 370–430 cm<sup>−1</sup> (Figure 9A) and the total <sup>34</sup>S shift is −7.5 cm<sup>−1</sup> (Table 4). In contrast, the four isotope-sensitive modes in Z<sub>ox</sub> exhibit a total <sup>34</sup>S shift of −19.9 cm<sup>−1</sup> (Table 4), and these vibrational modes are separated over a much wider frequency range of 290–410 cm<sup>−1</sup> (Figure 9B). We estimate that the error of the total <sup>34</sup>S isotope shift for Z<sub>ox</sub> is ±2 cm<sup>−1</sup>, based on the uncertainty of the weak features. Strikingly similar RR behavior is observed for the di-μ-sulfido-bridged Fe<sub>2</sub>S<sub>2</sub>(Cys)<sub>4</sub> clusters in oxidized ferredoxin where replacement with [<sup>34</sup>S]sulfide bridges results in frequency shifts of −3 to −7 cm<sup>−1</sup> for vibrations ranging from 280 to 425 cm<sup>−1</sup> and a total <sup>34</sup>S shift of −24.4 cm<sup>−1</sup> (Figure 9C). Moreover, oxidized adrenodoxin, which is analogous to 2Fe-ferredoxin and Cu<sub>A</sub> in having two bridging sulfurs for each metal ion, also exhibits a total <sup>34</sup>S shift of −23.9 cm<sup>−1</sup>.<sup>47</sup> In contrast, 4Fe-ferredoxin, with each metal ion coordinated to three bridging sulfurs, displays a total shift of −38.8 cm<sup>−1</sup> upon replacement with [<sup>34</sup>S]sulfide bridges.<sup>48</sup> Thus, the pattern of sulfur-isotope shifts in the RR spectrum of Z<sub>ox</sub> (Figure 9B) is best explained by the presence of a bridging sulfide ligand. A terminal Cu – S<sup>2−</sup> moiety appears unlikely for three reasons: first, the total <sup>34</sup>S isotope shift would probably be significantly smaller, on the order of −8 cm<sup>−1</sup>, as in azurin; second, it would be more difficult to accommodate the extra electron density associated with S<sup>2−</sup>, as opposed to OH<sup>−</sup>, in the crystal structure; and third, there are currently no stable examples of terminal sulfides in late transition metal ion complexes.<sup>49</sup>

At least eight vibrational fundamentals between 200 and 450 cm<sup>−1</sup> are resonance enhanced (Figure 7A). A three-atom Cu<sub>2</sub>S structure can have only three normal modes of vibration, whereas a Cu<sub>4</sub>S structure can have nine normal modes, suggesting that the sulfide ligand may bridge all the copper ions in the Cu<sub>Z</sub> cluster. The observed electron density in the structure appears to be able to accommodate a sulfide ion, as opposed to

(45) Ling, J.; Nestor, L. P.; Czernuszewicz, R. S.; Spiro, T. G.; Fraczkiwicz, R.; Sharma, K. D.; Loehr, T. M.; Sanders-Loehr, J. *J. Am. Chem. Soc.* **1994**, *116*, 7682–7691.

(46) Kincaid, J.; Stein, P.; Spiro, T. G. *Proc. Natl. Acad. Sci. U.S.A.* **1979**, *76*, 549–552.

(47) Han, S.; Czernuszewicz, R. S.; Kimura, T.; Adams, M. W. W.; Spiro, T. G. *J. Am. Chem. Soc.* **1989**, *111*, 3505–3511.

(48) Czernuszewicz, R. S.; Macor, K. A.; Johnson, M. K.; Gewirth, A.; Spiro, T. G. *J. Am. Chem. Soc.* **1987**, *109*, 7178–7187.

(49) Vivic, D. A.; Jones, W. D. *J. Am. Chem. Soc.* **1999**, *121*, 4070–4071.

hydroxide, in the predicted bridging location. Since the assembly of the catalytic  $\text{Cu}_Z$  site requires intracellular-processing enzymes,<sup>3,50</sup> it is possible that the sulfide ligand is inserted during enzyme biogenesis. An alternative explanation, recently proposed by Farrar et al.<sup>19</sup> is that the  $Z_{\text{ox}}$  cluster is an altered form of the  $A_{\text{mv}}$  cluster, such that the two cysteine ligands conserved in standard sequence alignments are used in both the A and Z sites. Given the discovery of inorganic sulfide in  $\text{N}_2\text{OR}$ <sup>22</sup> and the possibility of other explanations for the results of Farrar et al., this hypothesis is unnecessary.

**Structure of the  $Z_{\text{mv}}$  Site.** In contrast to purple  $\text{Cu}_A$  sites, which typically display absorption bands at 480, 540, and 780 nm, the intensely blue  $Z_{\text{mv}}$  site in reduced  $\text{N}_2\text{OR}$  displays one strong absorption band at 650 nm. Excitation within this absorption band, as reported previously,<sup>14</sup> yields a RR spectrum with a dominant vibrational mode at  $382\text{ cm}^{-1}$  and seven weaker features in the  $250\text{--}400\text{ cm}^{-1}$  region (Figure 7D). The  $382\text{ cm}^{-1}$  frequency of the most intense Cu–S vibrational mode in  $Z_{\text{mv}}$  appears to differ from the  $352\text{--}$  and  $408\text{ cm}^{-1}$  values for  $Z_{\text{ox}}$ , but there are a number of similarities in their Raman spectral patterns. Thus,  $Z_{\text{mv}}$  exhibits significant  $^{34}\text{S}$  shifts ( $-2$  to  $-5.8\text{ cm}^{-1}$ ) in six vibrational modes that spread out over a frequency range of  $282\text{--}382\text{ cm}^{-1}$  (Figure 9B) and can again be assigned to a structure in which the sulfide bridges multiple copper ions in the  $\text{Cu}_Z$  cluster. No S–C stretch is apparent, as expected. The total  $^{34}\text{S}$  shift of  $-16.9\text{ cm}^{-1}$  for  $Z_{\text{mv}}$  (Table 4) is of a magnitude similar to the  $-19.9\text{ cm}^{-1}$  shift for  $Z_{\text{ox}}$  and is consistent with a bridged structure. As in the case of  $Z_{\text{ox}}$ ,  $Z_{\text{mv}}$  exhibits a smaller degree of coordinate mixing than in the  $A_{\text{mv}}$  site of  $\text{N}_2\text{OR}$ , as evidenced by the smaller  $^{15}\text{N}(\text{His})$  shift of  $-1.6\text{ cm}^{-1}$  (Table 4). The C622D variant of  $\text{N}_2\text{OR}$ , which lacks one of the two conserved cysteine ligands, cannot form either  $A_{\text{mv}}$  or  $Z_{\text{ox}}$  but does form a  $Z_{\text{mv}}^*$  species (Figure 8D), which displays an RR spectrum almost identical to that of  $Z_{\text{mv}}$  in wild-type  $\text{N}_2\text{OR}$  (Figure 7D).

**Structure of the  $Z_{\text{mv}}^*$  Site.** An increase, relative to native  $\text{N}_2\text{OR}$ , in the absorption band at 650 nm in the aerobically isolated enzyme has previously been associated with a mixed-valence form of  $\text{Cu}_Z$  designated  $Z_{\text{mv}}^*$ . The similarities between  $Z_{\text{mv}}^*$  and  $Z_{\text{mv}}$  are striking (Table 5): identical absorbance maximums at 650 nm, nearly identical MCD features at 625 (+) and 660 nm (–), superimposable broad EPR signals, and RR spectra with nearly identical peak frequencies ( $\pm 1\text{ cm}^{-1}$ ) and intensities (Figure 7C,D). In light of these remarkable similarities,  $Z_{\text{mv}}$  and  $Z_{\text{mv}}^*$  are considered to be the same spectroscopic chromophore rather than independent moieties. Minor differences in their spectroscopic properties, as well as differences in their apparent sensitivities to various reagents such as ascorbate, dithionite, and oxygen,<sup>5,7</sup> most likely reflect changes in the microenvironments of the catalytic copper cluster. Such protein perturbations may result from the different pathways by which the site is initially produced, e.g., reduction by dithionite versus aerobic enzyme purification.

**A New Type of Copper Cluster in Biology.** The data reported herein, along with the analytical data for sulfide, strongly indicate that  $\text{Cu}_Z$  is a copper–sulfide cluster, the first such active-site center reported. Importantly, our results provide a link between the designation of  $\text{Cu}_Z$  as the catalytic site<sup>4,22,51</sup>

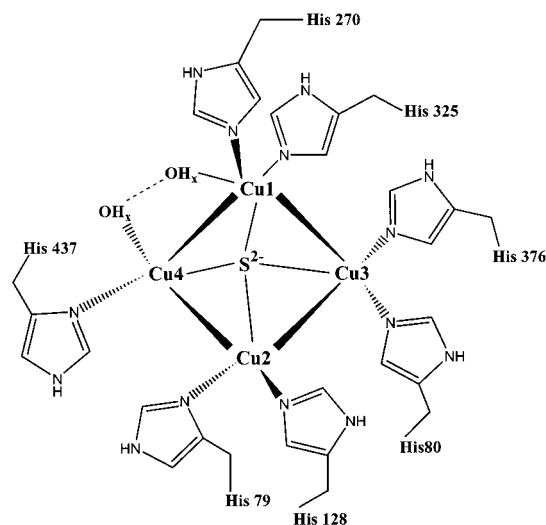


**Figure 10.** Model of the  $\text{Cu}_Z$  site in nitrous oxide reductase based on the X-ray crystal structure,<sup>4</sup> sulfur analyses,<sup>22</sup> and the spectroscopic data presented herein.

and the “spectroscopic”  $\text{Cu}_Z$ .<sup>7</sup> The significantly different vibrational frequencies and intensities in  $Z_{\text{ox}}$  and  $Z_{\text{mv}}$ , relative to those in  $\text{Cu}_A$ , are readily rationalized as reflecting the structural differences between the two types of clusters, e.g., sulfido bridging as compared to thiolate bridging. Moreover, several other aspects of the RR data argue strongly for substantial structural differences between  $\text{Cu}_A$  and  $\text{Cu}_Z$ : (1) the absence of a cysteine S–C stretch in the RR spectrum of  $Z_{\text{ox}}$  and  $Z_{\text{mv}}$  (Tables 1 and 2); (2) the smaller number of vibrational modes in  $\text{Cu}_Z$  (7 or 8 versus 10 in  $A_{\text{mv}}$ ); (3) the total magnitude of the  $^{15}\text{N}(\text{His})$  shift, only  $-0.9\text{ cm}^{-1}$  in  $Z_{\text{ox}}$  and  $-1.6$  in  $Z_{\text{mv}}$ , considerably smaller than the value of  $-4.5\text{ cm}^{-1}$  for the  $A_{\text{mv}}$  site in  $\text{N}_2\text{OR}$  (Table 4).

It is intriguing that an unprecedented type of copper site—a  $\text{Cu}_4\text{S}$  cluster—is utilized to catalyze one of the most difficult redox reactions in biology—the reduction of nitrous oxide to dinitrogen (eq 2). A schematic representation of  $\text{Cu}_Z$  based on the structure,<sup>4</sup> the analytical data,<sup>22</sup> and the results herein is shown in Figure 10. Clearly nitrous oxide reductase has again provided the inorganic biochemistry community a host of fascinating new questions to explore as we endeavor to elucidate the structure/reactivity correlations of the unique catalytic cluster and the molecular details of the structure, mechanism, and biosynthesis of  $\text{N}_2\text{OR}$ . These results also provide a very satisfying link between the crystal structure and the spectroscopy of  $\text{N}_2\text{OR}$ . We can now confidently assign the electronic transitions, vibrational frequencies, and EPR signals of  $\text{N}_2\text{OR}$  to either  $\text{Cu}_A$  or  $\text{Cu}_Z$ , thereby facilitating detailed studies of the relationships between active-site structure and function.

**Role of the  $\text{Cu}_A$  Site in Electron Transfer.** A low reorganization energy is important for minimizing the kinetic barrier of a redox reaction and thereby facilitating rapid electron transfer.<sup>52</sup> Multinuclear clusters such as  $\text{Cu}_A$  sites lower the reorganization energy by delocalizing the change in charge over multiple metal centers<sup>53</sup> and by maintaining a relatively rigid metal ion geometry that is favorable to both oxidation states. For example, EXAFS studies of  $\text{CuO Cu}_A$  have shown that very little change in  $\text{Cu}_2\text{S}_2$  cluster geometry occurs upon one-electron reduction.<sup>54</sup> Resonance Raman studies have shown that all  $\text{Cu}_A$ -containing proteins and engineered constructs display common

(50) Zumft, W. G.; Kroneck, P. M. H. In *Mechanisms of Metallocenter Assembly*; Hausinger, R. P., Eichorn, G. L., Marzilli, L. G., Eds.; VCH Publishers: New York, 1996; pp 193–221.

(51) Prudêncio, M.; Pereira, A. S.; Besson, S.; Cabrito, I.; Brown, K.; Samyn, B.; Devreese, B.; Van Beeumen, J.; Rusnak, F.; Fauque, G.; Moura, J. J. G.; Tegoni, M.; Cambillau, C.; Moura, I. *Biochemistry* **2000**, *39*, 3899–3907.

(52) Ramirez, B. E.; Malmström, B. G.; Winkler, J. R.; Gray, H. B. *Proc. Natl. Acad. Sci. U.S.A.* **1995**, *92*, 11949–11951.

(53) Beinert, H. *Eur. J. Biochem.* **1997**, *245*, 521–532.

vibrational features reflective of a rigid  $\text{Cu}_2\text{Cys}_2\text{His}_2$  core.<sup>15,32</sup> Kinetic studies of a  $\text{Cu}_A$  construct in azurin have shown that this engineered  $\text{Cu}_A$  site increases the rate of electron transfer 3-fold relative to the mononuclear Cu site in native azurin and lowers the reorganization energy by 50%.<sup>55</sup> The present RR data on the  $\text{Cu}_A$  site of  $\text{N}_2\text{OR}$  reveals a greater coupling of the Cu—S stretch with cysteine and histidine vibrations than in the  $\text{Cu}_A$  site of CcO. This coupling probably reflects an even greater rigidity for the  $\text{Cu}_A$  cluster in  $\text{N}_2\text{OR}$ , perhaps enhancing its effectiveness as an electron-transfer catalyst.

Loss of the  $\text{N}_2\text{OR}$  catalytic site, as in the case of the  $\text{Cu}_A$ -only variant (where  $\text{Cu}_A$  accounts for all the copper in the protein), causes subtle spectroscopic perturbations in the  $\text{Cu}_A$  site. These changes are manifested as slight differences in the relative intensities, but not frequencies, of the RR vibrational modes. EPR and ENDOR studies suggest a lower symmetry in the  $\text{Cu}_A$  site in the  $\text{N}_2\text{OR}$  variant, relative to that found in native enzyme.<sup>10</sup> The disturbance of this site, upon loss of the catalytic

(54) Blackburn, N. J.; de Vries, S.; Barr, M. E.; Houser, R. P.; Tolman, W. B.; Sanders, D.; Fee, J. A. *J. Am. Chem. Soc.* **1997**, *119*, 6135–6143.

(55) Farver, O.; Lu, Y.; Ang, M. C.; Pecht, I. *Proc. Natl. Acad. Sci. U.S.A.* **1999**, *96*, 899–902.

(56) Han, S.; Czernuszewicz, R.; Kimura, T.; Adams, M. W. W.; Spiro, T. G. *J. Am. Chem. Soc.* **1989**, *111*, 3505–3512.

site, is understandable in terms of the proximity of the  $\text{Cu}_Z$  site in one subunit to the  $\text{Cu}_A$  in the other. As pointed out, the  $\text{N}_2\text{-OR}$  structure strongly suggests that  $\text{Cu}_A$  functions as the electron acceptor from physiological donors and likely undergoes two redox cycles during catalysis.

**Abbreviations:**  $\text{N}_2\text{OR}$ , nitrous oxide reductase; CcO, cytochrome *c* oxidase; RR, resonance Raman; EPR, electron paramagnetic resonance; ENDOR, electron nuclear double resonance; EXAFS, extended X-ray absorption fine structure; CD, circular dichroism; MCD, magnetic circular dichroism; NCA, normal coordinate analysis.

**Acknowledgment.** This work was supported by grants from the NSF [MCB-9723715 (D.M.D.)], the NIH [GM-18865 (J.S.-L.)], and the *Deutsche Forschungsgemeinschaft* and *Fonds der Chemischen Industrie* (W.Z.). We thank the Stable Isotope Resource at Los Alamos National Laboratory for providing the  $^{15}\text{N}$ -enriched histidine (supported by NIH Grant RR02231, under the auspices of the U.S. Department of Energy). We also thank Drs. Roman Czernuszewicz, Jaqueline Farrar, and Andrew Thomson for sharing data prior to publication, and Thomas M. Loehr for numerous helpful discussions.

JA994322I